Fraunhofer Institut
Techno- und
Wirtschaftsmathematik

V. Starikovicius

The multiphase flow and heat transfer in porous media

Berichte des Fraunhofer ITWM, Nr. 55 (2003)

ISSN 1434-9973

Bericht 55 (2003)

Die Veröffentlichungen in der Berichtsreihe des Fraunhofer ITWM können bezogen werden über:

Fraunhofer-Institut für Techno- und
Wirtschaftsmathematik ITWM
Gottlieb-Daimler-Straße, Geb. 49

67663 Kaiserslautern

Telefon: +49 (0) 6 31/2 05-32 42
Telefax: +49 (0) 6 31/2 05-41 39
E-Mail: info@itwm.fraunhofer.de
Internet: www.itwm.fraunhofer.de

Vorwort

Das Tätigkeitsfeld des Fraunhofer Instituts für Techno- und Wirtschaftsmathematik ITWM umfasst anwendungsnahe Grundlagenforschung, angewandte Forschung sowie Beratung und kundenspezifische Lösungen auf allen Gebieten, die für Techno- und Wirtschaftsmathematik bedeutsam sind.

In der Reihe »Berichte des Fraunhofer ITWM« soll die Arbeit des Instituts kontinuierlich einer interessierten Öffentlichkeit in Industrie, Wirtschaft und Wissenschaft vorgestellt werden. Durch die enge Verzahnung mit dem Fachbereich Mathematik der Universität Kaiserslautern sowie durch zahlreiche Kooperationen mit internationalen Institutionen und Hochschulen in den Bereichen Ausbildung und Forschung ist ein großes Potenzial für Forschungsberichte vorhanden. In die Berichtreihe sollen sowohl hervorragende Diplom- und Projektarbeiten und Dissertationen als auch Forschungsberichte der Institutsmitarbeiter und Institutsgäste zu aktuellen Fragen der Techno- und Wirtschaftsmathematik aufgenommen werden.

Darüberhinaus bietet die Reihe ein Forum für die Berichterstattung über die zahlreichen Kooperationsprojekte des Instituts mit Partnern aus Industrie und Wirtschaft.

Berichterstattung heißt hier Dokumentation darüber, wie aktuelle Ergebnisse aus mathematischer Forschungs- und Entwicklungsarbeit in industrielle Anwendungen und Softwareprodukte transferiert werden, und wie umgekehrt Probleme der Praxis neue interessante mathematische Fragestellungen generieren.

Prof. Dr. Dieter Prätzel-Wolters
Institutsleiter

Kaiserslautern, im Juni 2001

The multiphase flow and heat transfer in porous media

Vadimas Starikovičius

Vilnius University, Faculty of Mathematics and Informatics
Naugarduko 24, LT-2600 Vilnius, Lithuania

Vilnius Gediminas Technical University, Computing Center
Saultekio 11, LT-2040 Vilnius, Lithuania

e-mail: vs@sc.vtu.lt

Abstract

In first part of this work, summaries of traditional Multiphase Flow Model and more recent Multiphase Mixture Model are presented. Attention is being paid to attempts include various heterogeneous aspects into models. In second part, MMM based differential model for two-phase immiscible flow in porous media is considered. A numerical scheme based on the sequential solution procedure and control volume based finite difference schemes for the pressure and saturation-conservation equations is developed. A computer simulator is built, which exploits object-oriented programming techniques. Numerical result for several test problems are reported.

Keywords: Two-phase flow in porous media, various formulations, global pressure, multiphase mixture model, numerical simulation

1 Introduction

The multiphase flow in porous media has gained and is still gaining a lot of attention. This is due to the fact that problems involving the multiphase flow, heat transfer, and multicomponent mass transport in porous media arise in a broad spectrum of engineering disciplines. Important technological applications include the drying of porous solids and soils [24], subsurface contamination and remediation [2], thermally enhanced oil recovery [58], geothermal energy production [5], porous heat pipes [28], multiphase trickle bed reactors [57], nuclear reactor safety analysis [59], high-level radioactive waste repositories [60], paper machines [61].

However, due to the complicated transport phenomena involved, the multiphase flow and heat transport in porous media remain poorly understood and analytically intractable. Over the last decades a lot of efforts was made to create fundamental mathematical models for those phenomena. One of the purposes

of this research is to review and to summarize the recent studies in this field and to compile the hierarchy of the models in order to provide a basis for further model developments and applications to specific problems.

Traditionally multiphase flow in porous media has been approached by so-called Multiphase Flow Model (MFM) [1, 4], in which various phases are considered as distinct fluids with individual thermodynamic and transport properties and with different flow velocities. The transport phenomena are mathematically described by the basic principles of conservation for each phase separately and by appropriate interfacial conditions between various phases. The generalized Darcy's law is employed to represent momentum conservation in each phase, with the relative permeabilities of each phase introduced to account for a decrease in effective flow cross-section due to the presence of other fluids. The governing macroscopic equations of this model are summarized in section 2.

The closure conditions of the model are considered in section 3. We review the existing literature and present the summary of constitutive relationships and state equations for various applications. An attention is being paid to the attempts to account in the model for the effects of porous medium heterogeneity.

Due to the inherent nonlinearities of multiphase flow problems, exact solutions of MFM are limited to a small class of problems in one dimension and with numerous simplifying assumptions, e.g. Buckley-Leverett case [16]. Solving practical problems, which usually involve multi-dimensional effects, gravity, capillarity and phase change, requires a solution of multiply coupled sets of nonlinear differential equations. For this reason, there has been a great number of studies to develop robust numerical algorithms [6, 9, 11, 17], approximate models [18], and different reformulations like the fractional flow model [7].

Moreover, the presence of the moving and irregular interfaces between the single- and two-phase regions adds more difficulties in the numerical solution. The locations of these interfaces are not known a priori, but must be determined by the coupled flows in adjacent regions. These difficulties can be avoided in the recently developed Multiphase Mixture Model (MMM) [20]. The model is single-domain formulation, because all governing equations are valid throughout a problem domain including single- and multiphase regions. In addition, the formulation strongly resembles the single-phase transport theory and, thus, is amenable to solutions by conventional numerical algorithms. It also requires much fewer nonlinear and coupled differential equations to be solved.

This model is presented in section 4. In subsection 4.5, we formulate a MMM based two-phase model for immiscible flow, which we will solve numerically later. This is not an extensive review of literature on existing models. However, for a more complete view of the hierarchy of the models, a simple approximated model called Unsaturated Flow Theory [18] is presented in section 5. The extensive reviews of multiphase flow studies are given in [2, 12, 18, 19, 24].

In section 6, we develop a numerical scheme for the solution of the two-phase model under consideration. Based on the analysis of the nonlinearity and coupling of the system, we utilize a sequential solution procedure to decouple the partial differential equations (PDEs). To preserve the important in the model property of the mass conservation, control volume based finite difference schemes are used to solve separate PDEs.

Thereafter, in section 7, we develop a computer simulator for the two-phase immiscible flow in porous media. The object-oriented programming technique from [13] is utilized to build a PDE system solver in a flexible manner, combin-

ing independent PDE solver objects. It shown how to handle various types of constitutive relationships.

Finally, in section 8, we test our differential model, numerical procedure and computer simulator in three particular cases: 1D Buckley-Leverett problem, 1D McWhorter, and 2D heterogeneous Buckley-Leverett problem.

2 Multiphase flow model (MFM)

A brief summary of the MFM for multiphase, multicomponent transport in a porous medium is given below. In this model, phases are considered as distinct fluids with individual thermodynamic and transport properties. The following set of governing macroscopic equations can either semiempirically postulated [4] or derived by the volume averaging method [1].

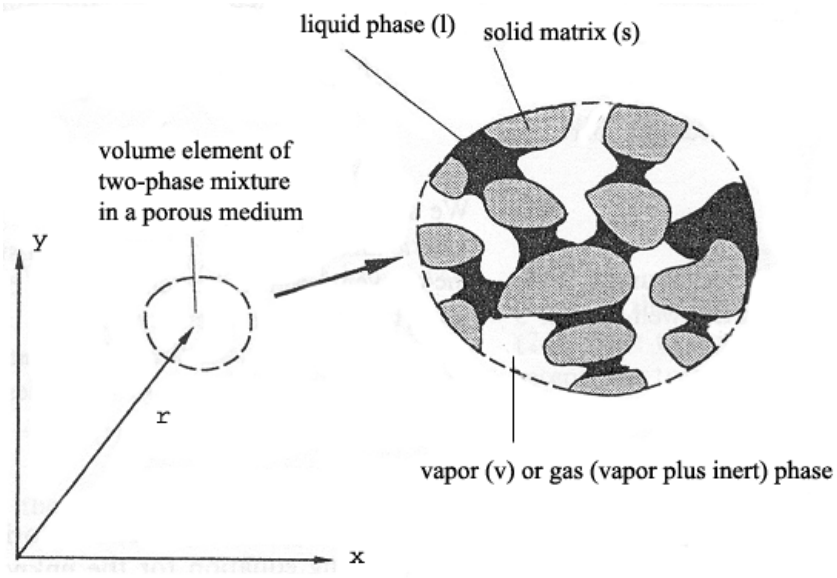

Figure 1: Schematic illustration of a control volume in multiphase system.

In latter case, the macroscopic equations are obtained by taking the average of the microscopic equations over the representative elementary volume (control volume). The microscopic equations are the equations of momentum, mass and energy conservation in all considered phases and at the interfaces. The control volume should be larger than the maximum dimension of any phase element, but much smaller than the characteristic scale of the system (Figure 1). Such scale changing enables to convert the real discontinuous medium to a fictitious continuous equivalent one. Each macroscopic term is obtained by averaging microscopic one. The averaging (integration) is done by using various closing assumptions (homogeneity, periodic cell structure etc.) [24].

Here are the governing equations of MFM for multiphase, multicomponent transport in a non-deformable porous medium:

1. *Mass conservation in phase k*:

$$\varepsilon \frac{\partial (\rho_k s_k)}{\partial t} + \nabla \cdot (\rho_k \mathbf{u}_k) = \bar{m}_k, \tag{1}$$

where ε is the porosity of porous medium, ρ_k is the phase density, s_k is the phase saturation denoting the volumetric fraction of the void space occupied by phase k,

$$\sum_k s_k = 1, \tag{2}$$

and $\mathbf{u}_k$ is the superficial (or Darcian) velocity vector (volume rate of flow through a unit cross-sectional area of multiple fluids and porous medium). It is also called bulk velocity. The term $\bar{m}_k$ represents an interfacial mass transfer rate from all other phases to phase k. In the absence of any external mass source or sink, it follows that

$$\sum_k \bar{m}_k = 0. \tag{3}$$

It is assumed that the porous medium is not deformable.

2. *Momentum conservation in phase k*:

$$\mathbf{u}_k = -\mathbf{K} \frac{k_{rk}}{\mu_k} (\nabla p_k - \rho_k \mathbf{g}), \tag{4}$$

where $\mathbf{K}$ is the absolute permeability tensor of porous medium, k_{rk} is the relative permeability of phase k, μ_k is the phase dynamic viscosity, p_k is the phase pressure, and $\mathbf{g}$ is the acceleration vector due to gravity. The difference between the pressures for two adjacent phases k and j is called a capillary pressure

$$p_{c\,kj} = p_k - p_j. \tag{5}$$

This generalized Darcy's law is valid if inertia as well as (macroscopic) viscous, boundary effects can be neglected, for example if velocities of fluids are quite small. In other case, well-established expressions from analogy with Navier-Stokes equation should be used [12, 14, 25]. For example, a quadratic inertia term is often introduced for modeling the inertia effect. However, much more fundamental research on multiphase flows in porous media is needed to rigorously include these non-Darcian effects into the model.

3. *Mass conservation of component α in phase k*:

$$\frac{\partial}{\partial t} (\varepsilon \rho_k s_k C_k^\alpha) + \nabla \cdot (\rho_k \mathbf{u}_k C_k^\alpha) = -\nabla \cdot \mathbf{j}_k^\alpha + \bar{J}_k^\alpha, \tag{6}$$

where C_k^α is the mass concentration of component (species) α in phase k,

$$\sum_\alpha C_k^\alpha = 1, \tag{7}$$

and $\mathbf{j}_k^\alpha$ is an average flux vector which represents the nonadvective (diffusive) flux of component α in phase k due to molecular diffusion and/or hydrodynamic dispersion. It is usually expressed in Fickian form:

$$\mathbf{j}_k^\alpha = -\varepsilon \rho_k s_k \mathbf{D}_k^\alpha \nabla C_k^\alpha, \tag{8}$$

where $\mathbf{D}_k^\alpha$ is a macroscopic second-order tensor incorporating both diffusive and dispersive effects. The last term $\bar{J}_k^\alpha$ in equation (6) denotes the interface transfer rate of component α caused by chemical reaction (chemical nonequilibrium) and/or phase change at the interfaces between phase k and all other phases. Recognizing that production of component α in phase k must be accompanied by destruction of component α in other phases, it follows that

$$\sum_k \bar{J}_k^\alpha = 0. \tag{9}$$

It is assumed that there is no external generation of components due to the chemical or biological reactions.

4. *Energy conservation in phase k*:

$$\frac{\partial}{\partial t}(\varepsilon \rho_k s_k h_k) + \nabla \cdot (\rho_k \mathbf{u}_k h_k) = \nabla \cdot (\varepsilon s_k k_k \nabla T) + \bar{q}_k, \tag{10}$$

where local thermal equilibrium among phases has been assumed ($T_k = T$, $\forall\ k$), and k_k and $\bar{q}_k$ represent the effective thermal conductivity of phase k and interphase heat transfer rate associated with phase k, respectively. Hence,

$$\sum_k \bar{q}_k = q, \tag{11}$$

where q is an external volumetric heat source or sink. The phase enthalpy h_k is related to common temperature T via

$$h_k = \int_0^T c_k \, dT + h_k^0, \tag{12}$$

where c_k and h_k^0 represent the effective specific heat and the reference enthalpy of phase k, respectively. The validity of the local thermal equilibrium assumption is discussed in [22, 23, 25]. One of conclusions in [22] is that the local thermal equilibrium assumption is not valid on the heat point (at the region where the evaporization takes place). Using the method of volume averaging, Kaviany [12] extensively examined local thermal nonequilibrium effects.

The above basic conservation laws provide a full system of governing equations for the unknown vector velocities $\mathbf{u}_k$, scalar pressures p_k, scalar saturations s_k, mass concentrations C_k^α, and the common temperature T.

3 Constitutive relationships

In general case, the averaging can be seen as a process of giving the guidance: while postulating, we can easily forget some terms, which on the other hand appear in averaging. However, it cannot eliminate completely the need in the postulation. To close the system, we need an additional set of equations.

The constitutive relationships specify how the phases interact with themselves, with each other and with porous medium. The state equations specify the thermodynamic state of the phases as functions of those state variables that

determine it. The closure conditions are usually determined by experiments. Commonly, these experiments are made for very specific flows and flow situations and may be often valid only for specific application in a narrow range of flow conditions and concentrations. In this section, we review the existing literature and present the summary of constitutive relationships and state equations for various applications.

The capillary pressure functions are dependent only on the pore geometry, fluids physical properties and phase saturations [26], i.e.

$$p_{c\,kj} = fn(\varepsilon, \sigma_{kj}, s_1, s_2, \ldots, s_k, \ldots), \tag{13}$$

where σ_{kj} is the interfacial tension at the $k-j$ interface. The capillary pressure functions are generally multi-valued and exhibit hysteretic behaviors.

The two-phase capillary pressure can be expressed by a Leverett dimensionless function $J(S)$ as follows [27]:

$$p_c = \sigma \left(\frac{\varepsilon}{\mathbf{K}}\right)^{1/2} J(S), \tag{14}$$

where S is the normalized liquid saturation and is defined as

$$S = \frac{s - s_r}{s_m - s_r}. \tag{15}$$

The variable s_r is the irreducible (residual) saturation. At this saturation, the liquid becomes immobile since no interpore connections of liquid exist. The variable s_m is the maximum achievable liquid saturation. In many cases, s_m is less than unity. Expression (14) implies that the characteristic pore dimension is proportional to $(\mathbf{K}/\varepsilon)^{1/2}$ [28].

In gas-liquid systems, the experimentally obtained J-values typically lie between two limiting curves, known as drainage and imbibition curves. The drainage curve is obtained when the porous medium is undergoing draining of the wetting liquid and the liquid saturation decreases. On the other hand, the imbibition curve corresponds to measurements conducted when the porous medium is undergoing imbibition (wetting) and the liquid saturation increases.

In the literature, drainage data, imbibition data or an average curve between these two limits has been employed. Udell [28] correlated imbibition capillary pressure data obtained by Leverett [27] with

$$J = 1.417(1-S) - 2.120(1-S)^2 + 1.263(1-S)^3 \tag{16}$$

for applications in drying and porous heat pipes. In contrast, Grosser [29] used the drainage data to obtain

$$J = 0.48 + 0.036 \ln\left(\frac{1-S}{S}\right) \tag{17}$$

for application to the analysis of transient two-phase flow in a trickle reactor and packed beds. In nuclear reactor safety analysis, both drainage and imbibition capillary pressure data are correlated to obtain the following widely used J-function

$$J = \frac{(S^{-1}-1)^{0.175}}{\sqrt{5}}. \tag{18}$$

Also, currently are widely used the empirical relations for capillary pressure from van Genuchten [30]:

$$p_c = p_0(S^{-1/m} - 1)^{1-m}, \tag{19}$$

and Brooks and Corey [31]:

$$p_c = p_d S^{-1/\lambda}, \tag{20}$$

where p_0 is characteristic capillary pressure, p_d is called entry pressure, parameters m $(0 < m < 1)$ and λ $(0.2 < \lambda < 3)$ are related to the distribution of pore sizes. The narrow range of pore sizes corresponds to the large m and small λ and vice versa for a highly non-uniform material.

The three-phase capillary pressure functions can be developed from two-phase relationships, as discussed by Parker [32].

The relative permeabilities are assumed to be known functions of the phase saturations, which must be empirically determined. In the literature, the simplest correlations used for the relative permeabilities are the power functions of phase saturations, i.e. for two-phase flow

$$k_{rl} = S^n, \qquad k_{rg} = (1 - S)^n. \tag{21}$$

For example, linear functions $(n = 1)$ of relative permeabilities are usually employed for geothermal systems due to their simplicity and accuracy [33]. Cubic forms $(n = 3)$ are widely used in petroleum and nuclear safety engineering, porous heat pipes [34].

Again in the literature, often are utilized the expressions for relative permeabilities from van Genuchten [30]:

$$k_{rl} = S^{1/2}\left(1 - \left(1 - S^{1/m}\right)^m\right)^2, \qquad k_{rg} = (1 - S)^{1/2}\left(1 - S^{1/m}\right)^{2m}, \tag{22}$$

and Brooks and Corey [31]:

$$k_{rl} = S^{\frac{2+3\lambda}{\lambda}}, \qquad k_{rg} = (1 - S)^2\left(1 - S^{\frac{2+\lambda}{\lambda}}\right). \tag{23}$$

The diffusive and/or dispersive mixing of fluids or components is often critical to the multiphase, multicomponent flow processes and must be understood and modeled accurately. The effective mass diffusivity tensor $\mathbf{D}_k^\alpha$ from Fick law (8) is usually complicated function of the thermophysical properties of the fluids and solid matrix, phase velocities, pore geometry and phase saturations. While there is no general formula, correlations for specialized situations are abundant in existing literature [35, 36].

In isotropic two-phase, binary (liquid-gas) systems, the mass diffusivity coefficient of component can be obtained as follows [20]:

$$D_k = \tau_k D_k^m + D_k^d, \tag{24}$$

where τ_k is the phase k tortuosity, D_k^m is the molecular diffusion coefficient and D_k^d is component's dispersion coefficient in phase k. Usually, all these values are obtained empirically or some effects are neglected.

Presently, much effort is being expended to model the hydrodynamic dispersion or mechanical mixing caused by velocity variations and flow through

heterogeneous medium [37]. For single-phase flow in porous media, Koch and Brady [38] obtained expression for the species dispersion coefficient. The dispersion tensor has strong velocity dependence [39].

The interfacial mass transfer between phases is also an object of intensive studies. Usually, it is determined experimentally for specific applications [22, 40]. However, recently, some macroscopic multiphase flow models have been developed that rigorously account for interfacial mass transfer [14, 41].

Until recently, the effects of porous medium heterogeneity on multiphase flow have not been systematically addressed and they are currently poorly understood. Much work must be done in volume averaging or homogenizing of terms like porosity and permeability to rigorously include these effects in the macroscopic models. Statistical methods have also shown promise in this area [42, 43].

In many applications, the porosity of the matrix may not be uniform. Due to so called channeling effect, the porosity is high near to the impermeable boundary and decreases to an asymptotic value at about four to five sphere diameters from it. A common practice to approximately simulate the porosity variation is to consider an exponential decaying function dependent on distance from the wall [25, 44]:

$$\varepsilon(x) = \varepsilon_\infty \left[1 + a_1 \exp\left(\frac{-a_2 x}{d_p}\right)\right], \tag{25}$$

where ε_∞ is the free steam porosity, d_p is mean particle diameter, a_1 and a_2 are empirical constants. These models are single-phase and in the momentum equation account for the inertial and boundary effects. The porosity variation can be rigorously predicted by accounting for the damped oscillation close to the wall. In the literature, the models with random porosity distribution are proposed [44, 45].

In geothermal systems or porous layers formed after a nuclear accident, porosity may vary with depth due to variation of the weight of overlying material and/or differential settling of different particle sizes. In the such and similar cases, when porosity varies sufficiently weak, the Darcy's law can be used. This expected to be true when the distance over which the porosity varies significantly is large compared with the pore size. This can be expressed mathematically as

$$\frac{\varepsilon}{d\varepsilon/dx} \gg d_p. \tag{26}$$

Chuah and Carey [46] proposed an exponential porosity profile for bottom heating of a liquid-saturated porous medium whose porosity varies with height:

$$\varepsilon(x) = \varepsilon_\infty \left[1 - \gamma \exp\left(\frac{x}{L}\right)\right], \tag{27}$$

where

$$\gamma = \frac{\varepsilon_\infty - \varepsilon_0}{\varepsilon_\infty}. \tag{28}$$

The constants ε_∞ and ε_0 are the ambient porosity and the porosity at the heating surface, respectively. Parameter L is the length of strong porosity variation layer near the heating surface.

In the model, the influence of the non-uniform porosity on the two-phase transport is also included in the capillary pressure function (14) and permeability. It is assumed there that permeability $\mathbf{K}$ can be expressed in terms of

porosity using the Kozeny-Carman formula [47]

$$\mathbf{K} = \frac{d_p^2 \varepsilon^3}{180(1-\varepsilon)^2}. \tag{29}$$

Although this relation strictly applies only to a packed bed of spheres, it is assumed to be qualitatively similar to the dependence of $\mathbf{K}$ on ε for other porous structures.

Effects of heterogeneity on vapor-liquid counterflow were studied in [48]. In the model, the same key assumption is used that capillarity and permeability are interrelated and saturation and permeability are decoupled in capillary pressure function (14). More detailed discussion about this assumption is in [49].

Another assumption, commonly made in the models, is that the gas (vapor) phase is ideal from thermodynamic view point. The modified state equations for an ideal gas are often used to eliminate the assumption of constant gas phase density [50, 21]. The gas phase density is expressed as a function of temperature and pressure.

Using Kelvin and Clapeyron equations, Udell [28] determined the temperature in the single-component two-phase zone as follows:

$$T = \frac{T_0 \left[1 + \frac{p_c}{h_{fg}\rho_l}\right]}{1 - \frac{RT_0}{h_{fg}} \ln \frac{p_v}{p_0}}, \tag{30}$$

where T_0 and p_0 are the reference temperature and its saturation pressure at which the capillary pressure is zero and hence the vapor pressure p_v becomes equal to the reference p_0, h_{fg} is the latent heat of liquid-vapor phase change (evaporation), R is the gas constant. The subscripts l and v denote liquid and vapor phases, respectively. The temperature in the two-phase zone is practically constant under most conditions except geothermal situations, where the relevant length scale is on the order of kilometers and hence the pressure variation is substantial [51]. Therefore, a single-component two-phase region can be often assumed to be isothermal without much loss of accuracy.

Completely different situation is in the case of multicomponent systems. In binary and multicomponent systems, the various phases can be of different compositions and co-exist in equilibrium over a range of temperatures, thus leading to a nonisothermal multiphase zone. Hence, the isothermal assumption cannot be made and energy conservation equations should be used in the models. In case of binary mixtures with a noncondensable gas, equation (30) for the equilibrium temperature in a two-phase zone is modified as [52]

$$T = \frac{T_0 \left[1 + \frac{p_c - y p_g}{h_{fg}\rho_l}\right]}{1 - \frac{RT_0}{h_{fg}} \ln \frac{p_g(1-y)}{p_0}}, \tag{31}$$

where vapor partial pressure is expressed by $p_g(1-y)$, with p_g being the gas phase pressure and y being the molar fraction of the noncondensable gas.

4 Multiphase mixture model (MMM)

Recently, an alternative approach was developed to the modeling of multiphase, multicomponent flow in porous media [20]. A key idea in the multiphase mixture

model is a concept of the multiphase mixture, which is considered as a single fluid consisting of diffusing constituents (phases). Multiphase flow is then described in terms of mixture properties and characteristics (density, velocity and etc.) by set of conservation equations, which are derived from classical MFM. Also, explicit relations describing the relative motions between the multiphase mixture and individual phase are obtained and can be used to determine the individual phase variables from the mixture variables. Therefore, no phase characteristics are lost. Next, the derivation of MMM is presented, which essentially follows [20] with some additional aspects introduced, namely, conditions for mixture pressure formulation.

4.1 Basic definitions

As in a classic multicomponent mixture, all physical properties of the multiphase mixture are consequences of the properties of its components. The mixture density and velocity are defined, respectively, as

$$\rho = \sum_k \rho_k s_k, \tag{32}$$

$$\rho\,\mathbf{u} = \sum_k \rho_k \mathbf{u}_k. \tag{33}$$

The superficial velocity of phase k, $\mathbf{u}_k$, is related to its intrinsic velocity by the phase volume fraction, and thus equation (33) implies that the mixture velocity $\mathbf{u}$ is a mass-weighted average of the intrinsic phase velocities multiplied by the porosity.

Analogically, the mixture species α concentration and enthalpy are defined, respectively, as

$$\rho\, C^\alpha = \sum_k \rho_k s_k C_k^\alpha, \tag{34}$$

$$\rho\, h = \sum_k \rho_k s_k h_k. \tag{35}$$

We note that C^α is a mass-averaged mixture concentration of species (component) α over all phases and from equation (7), it follows that

$$\sum_\alpha C^\alpha = 1. \tag{36}$$

The mixture kinematic viscosity is given by

$$\nu = \left(\sum_k \frac{k_{rk}}{\nu_k} \right)^{-1}, \tag{37}$$

where $\nu_k = \mu_k / \rho_k$ is the kinematic viscosity of phase k. The mobility of each phase in the multiphase mixture is defined as

$$\lambda_k = \frac{k_{rk}}{\nu_k}\nu, \quad \sum_k \lambda_k = 1. \tag{38}$$

In the literature, λ_k are often called the fractional flow functions.

The definition of the mixture pressure is somewhat nonconventional. To simplify the momentum conservation equation for the multiphase mixture, the mixture pressure is defined so that the following differential equation holds:

$$\nabla p = \sum_j \lambda_j \nabla p_j = \nabla p_k + \sum_j \lambda_j \nabla p_{c\,jk}. \tag{39}$$

At this point, we would like to state that it is not always possible to define such pressure function, especially, in heterogeneous, multidimensional, multiphase cases. As an example, let us consider two-dimensional two-phase flow. The mixture pressure function p will satisfy total differential condition: $\frac{d^2p}{dx\,dy} = \frac{d^2p}{dy\,dx}$, if and only if the following condition is satisfied:

$$\frac{d\lambda_2}{dy}\frac{dp_c}{dx} = \frac{d\lambda_2}{dx}\frac{dp_c}{dy}. \tag{40}$$

Note that it is always satisfied only in homogeneous case. Another example is a three-phase flow, when mixture pressure is function of two saturations $p(s_1, s_2)$. Total differential conditions for mixture pressure p result in the restrictions on such constitutive relationships of the model like relative permeabilities and capillary pressure functions. Therefore, arguing with [20], we state that MMM is not mathematically equivalent to MFM.

The explicit definition of the mixture pressure follows after the integration of equation (39). For a two-phase flow in homogeneous porous media, the mixture pressure can be defined as

$$\begin{aligned} p &= p_1 + \int_{S_c}^{S} \lambda_2(\xi)\frac{dp_c}{d\xi}d\xi = p_2 - \int_{S_c}^{S} \lambda_1(\xi)\frac{dp_c}{d\xi}d\xi = \\ &= \frac{p_1 + p_2}{2} + \frac{1}{2}\int_{S_c}^{S} \left(\lambda_2(\xi) - \lambda_1(\xi)\right)\frac{dp_c}{d\xi}d\xi, \end{aligned} \tag{41}$$

where S_c: $p_c(S_c) = 0$. In the literature, the last expression is called global pressure. It was introduced by Chavent [53].

4.2 Model equations

1. *Mass conservation of the multiphase mixture.*

   Adding the phase mass conservation equations (1) and applying constrain (3), the following equation is obtained:

   $$\varepsilon\frac{\partial \rho}{\partial t} + \nabla \cdot (\rho \mathbf{u}) = 0. \tag{42}$$

   This continuity equation is identical to the corresponding equation for a single-phase flow.

2. *Momentum conservation of the multiphase mixture.*

   First, using the definition (38) the phase momentum conservation equations (4) are transformed:

   $$\rho_k \mathbf{u}_k = -\mathbf{K}\frac{k_{rk}}{\nu_k}\left(\nabla p_k - \rho_k \mathbf{g}\right) = -\frac{\mathbf{K}}{\nu}\left(\lambda_k \nabla p_k - \lambda_k \rho_k \mathbf{g}\right). \tag{43}$$

Then, summing up these equations and using the definitions of the mixture velocity (33) and pressure (39), the momentum conservation equation of the multiphase mixture is obtained:

$$\rho\mathbf{u} = -\frac{\mathbf{K}}{\nu}\left(\nabla p - \left(\sum_k \lambda_k \rho_k\right)\mathbf{g}\right) = -\frac{\mathbf{K}}{\nu}\left(\nabla p - \gamma_\rho \rho \mathbf{g}\right), \tag{44}$$

where γ_ρ is called the density correction factor and is defined as

$$\gamma_\rho = \frac{\sum_k \lambda_k \rho_k}{\sum_k \rho_k s_k}. \tag{45}$$

This correction factor can be regarded as a property of the multiphase mixture. Physically, it means that the effective mixture density for gravitational force contains certain dynamic properties of phases (i.e. λ_k and hence ν_k) due to the relative motion among phases. In the case of single-phase flow, $\gamma_\rho = 1$. Similarly to MFM, modified momentum conservation equation from analogy with Navier-Stokes equation are used to include the non-Darcian effects into multiphase mixture model [54].

The diffusive mass flux of phase k within the multiphase mixture is defined as

$$\mathbf{j}_k = \rho_k \mathbf{u}_k - \lambda_k \rho \mathbf{u}, \qquad \sum_k \mathbf{j}_k = 0, \tag{46}$$

or alternatively,

$$\rho_k \mathbf{u}_k = \mathbf{j}_k + \lambda_k \rho \mathbf{u}. \tag{47}$$

Substituting the momentum equations for phase k (43) and for the mixture (44) into equation (46), the diffusive mass flux $\mathbf{j}_k$ can be expressed as follows:

$$\mathbf{j}_k = \frac{\mathbf{K}\lambda_k}{\nu}\sum_i \lambda_i \nabla p_{c\,ik} + \frac{\mathbf{K}\lambda_k}{\nu}\sum_i \lambda_i(\rho_k - \rho_i)\mathbf{g}. \tag{48}$$

The gradient of capillary pressure can be expressed through the gradients of saturations, concentrations, temperature and corresponding diffusion coefficients [19].

3. *Mass conservation of component α in the multiphase mixture.*

Adding the phase equations (6) and applying constrain (9) and definition (34), the following equation is obtained:

$$\varepsilon\frac{\partial}{\partial t}\left(\rho C^\alpha\right) + \nabla\cdot\left(\sum_k \rho_k \mathbf{u}_k C_k^\alpha\right) = -\nabla\cdot\left\{\sum_k \mathbf{j}_k^\alpha\right\}. \tag{49}$$

Using the phase velocity equation (47) and Fick law for the species diffusive flux (8), the above equation is transformed into

$$\varepsilon\frac{\partial}{\partial t}\left(\rho C^\alpha\right) + \nabla\cdot\left[\left(\sum_k \lambda_k C_k^\alpha\right)\mathbf{u}\right] = -\nabla\cdot\left\{\sum_k C_k^\alpha \mathbf{j}_k\right\} - \nabla\cdot\left\{\varepsilon\sum_k \rho_k s_k \mathbf{D}_k^\alpha \nabla C_k^\alpha\right\}. \tag{50}$$

Defining a correction factor for species advection and effective diffusion coefficient for the multiphase mixture, respectively, as

$$\gamma_c^\alpha = \frac{\rho \sum_k \lambda_k C_k^\alpha}{\sum_k \rho_k s_k C_k^\alpha}, \tag{51}$$

$$\rho \mathbf{D}^\alpha = \sum_k \rho_k s_k \mathbf{D}_k^\alpha, \tag{52}$$

the species conservation equation for the multiphase mixture is obtained in following form:

$$\varepsilon \frac{\partial}{\partial t}(\rho C^\alpha) + \nabla \cdot (\gamma_c^\alpha \rho \mathbf{u} C^\alpha) = \nabla \cdot (\varepsilon \rho \mathbf{D}^\alpha \nabla C^\alpha) + \nabla \cdot \left\{ \varepsilon \sum_k [\rho_k s_k \mathbf{D}_k^\alpha (\nabla C_k^\alpha - \nabla C^\alpha)] \right\} - \nabla \cdot \left\{ \sum_k C_k^\alpha \mathbf{j}_k \right\}. \tag{53}$$

This form is similar to a traditional species transport equation in a single-phase flow. The correction factor γ_c^α indicates that in the multiphase mixture, species α are advected by a modified velocity field $\gamma_c^\alpha \mathbf{u}$. The first two terms on the right-hand side of equation (53) represent the Fickian diffusion fluxes of component α within various phases and last term represents the diffusive fluxes of component α with various phases due to relative phase motions.

In the MMM, the phase compositions C_k^α are assumed to be known functions in the multiphase zone. They are given by the corresponding phase diagrams under the assumption of local chemical equilibrium [20, 21]. This assumption of interfacial equilibrium does not rule out the possibility of phase concentrations gradients on a macroscopic scale. It rather implies that contiguous phases reach a thermodynamic equilibrium very quickly(essentially immediately). And thus, the component's α mass concentration in the gas phase can be related to temperature and pressure through known equilibrium diagram, i.e.

$$C_g^\alpha = C_g^\alpha(T, p).$$

Therefore, solving all concentrations C^α from equations (53) determines through equations (34) all the phase saturations.

4. *Energy conservation for the multiphase mixture.*

Using local thermal equilibrium assumption, after summing up the phase energy equations (10) and using the constrain (11), we obtain

$$\frac{\partial}{\partial t}[(1-\varepsilon)\rho_s h_s + \varepsilon \rho h] + \nabla \cdot \left(\sum_k \rho_k \mathbf{u}_k h_k \right) = \nabla \cdot (k_{eff} \nabla T) + q, \tag{54}$$

where k_{eff} is an effective thermal conductivity of the composite system consisting of the solid matrix and the flowing multiphase mixture. The roughest estimation can be written as

$$k_{eff} = (1-\varepsilon)k_s + \varepsilon \sum_k s_k k_k. \tag{55}$$

Similarly, using the phase velocity equation (47) and defining a correction factor for energy advection as

$$\gamma_h = \frac{\rho \sum_k \lambda_k h_k}{\sum_k \rho_k s_k h_k}, \tag{56}$$

the energy conservation equation for the multiphase mixture is obtained in following form:

$$\frac{\partial}{\partial t}\left[(1-\varepsilon)\rho_s h_s + \varepsilon \rho h\right] + \nabla \cdot (\gamma_h \rho \mathbf{u} h) = \nabla \cdot (k_{eff} \nabla T) - \nabla \cdot \left[\sum_k (h_k \mathbf{j}_k)\right] + q. \tag{57}$$

Using enthalpy definition (12), this equation is often further transformed in the models [55, 56]. For example, substituting the identity

$$\nabla T = \frac{1}{c_j}\nabla h_j = \frac{1}{c_j}\nabla h + \frac{1}{c_j}\nabla (h_j - h), \tag{58}$$

where j denotes an arbitrary phase, into equation (57) yields

$$\frac{\partial}{\partial t}\left[(1-\varepsilon)\rho_s h_s + \varepsilon \rho h\right] + \nabla \cdot (\gamma_h \rho \mathbf{u} h) = \nabla \cdot \left(\frac{k_{eff}}{c_j}\nabla h\right) + \nabla \cdot \left[\frac{k_{eff}}{c_j}\nabla (h_j - h)\right] - \nabla \cdot \left[\sum_k (h_k \mathbf{j}_k)\right] + q. \tag{59}$$

At this point, we would like to propose an energy conservation equation for the multiphase mixture in terms of common temperature. Using the enthalpy definition (12) and the phase mass conservation equation (1), the phase energy conservation equation (10) can be rewritten as

$$\varepsilon \rho_k s_k c_k \frac{\partial T}{\partial t} + \rho_k c_k \mathbf{u}_k \cdot \nabla T + \bar{m}_k h_k = \nabla \cdot (\varepsilon s_k k_k \nabla T) + \bar{q}_k. \tag{60}$$

Summing up the above equations for all phases and solid matrix and using the constrain (11) and definition (55), we obtain

$$\left[(1-\varepsilon)\rho_s c_s + \varepsilon \rho c\right]\frac{\partial T}{\partial t} + \left(\sum_k c_k \rho_k \mathbf{u}_k\right) \cdot \nabla T + \sum_k \bar{m}_k h_k = \nabla \cdot (k_{eff} \nabla T) + q, \tag{61}$$

where ρc is the heat capacity of the multiphase mixture defined as

$$\rho c = \sum_k \rho_k s_k c_k. \tag{62}$$

Using the equation (47) to decompose the phase velocity and defining a correction factor for energy advection as

$$\gamma_c = \frac{\rho \sum_k \lambda_k c_k}{\sum_k \rho_k s_k c_k}, \tag{63}$$

the energy conservation equation for the multiphase mixture is obtained in following form:

$$[(1-\varepsilon)\rho_s c_s + \varepsilon\rho c]\frac{\partial T}{\partial t} + \gamma_c \rho c \mathbf{u}\cdot\nabla T + \sum_k \bar{m}_k h_k = \nabla\cdot(k_{eff}\nabla T) - \left(\sum_k c_k \mathbf{j}_k\right)\cdot\nabla T + q. \quad (64)$$

4.3 MMM solution procedure

Equations (42), (44), (53), and (57) provide a full system of governing equations for mixture variables, that is, mixture velocity $\mathbf{u}$, mixture pressure p, mixture concentrations C^α, and mixture temperature T. An advantage of MMM is that it requires much fewer nonlinear and coupled differential equations to be solved comparing with MFM. It avoids also such difficulties as the presence of the moving and irregular interfaces between the single- and multiphase regions. The model is single-domain formulation and all governing equations are valid throughout a whole problem domain including single- and multiphase regions. More detailed discussion about MMM and comparison with MFM is presented in [19]. In practical applications, the following solution procedure is used:

1. Using initial conditions, initial property coefficients of the multiphase mixture are evaluated.
2. The model's governing equations are solved and the mixture velocity, pressure, concentrations, and temperature fields are determined.
3. The thermodynamic state of each cell is determined and phase concentrations and saturations are then calculated using equilibrium phase diagrams.
4. The property coefficients are updated and the entire procedure is returned iteratively to step 2 until convergence is achieved.
5. Upon a converged solution is obtained, the individual phase variables (for example velocities) are calculated in a postprocessing fashion.

In order to solve the governing equations, we can use the fact, that they resemble the single-phase transport equations, and take an advantage of well established single-phase computational fluid dynamics (CFD) algorithms. For example, the SIMPLE (Semi-Implicit Method for Pressure-Linked Equations) algorithm of Patankar [62] can be revised for numerical solution of governing equations.

Successful calculations for several practical problems have been made [21, 54, 55, 56].

4.4 Application to two-phase binary systems

In this subsection, we consider an application of MMM to liquid-gas, binary systems. Examples of such systems include organic liquid-air during groundwater contamination [21], water-air in drying processes, and binary mixtures in heat pipes. Here is the set of conservation equations from section 4.2 for a two-phase, binary system:

mass conservation

$$\varepsilon \frac{\partial \rho}{\partial t} + \nabla \cdot (\rho \mathbf{u}) = 0, \tag{65}$$

momentum conservation

$$\rho \mathbf{u} = -\frac{\mathbf{K}}{\nu} \left(\nabla p - \gamma_\rho \rho \mathbf{g} \right), \tag{66}$$

species conservation

$$\begin{aligned} \varepsilon \frac{\partial}{\partial t} (\rho C) + \nabla \cdot (\gamma_c \rho \mathbf{u} C) &= \nabla \cdot (\varepsilon \rho \mathbf{D} \nabla C) \\ &+ \nabla \cdot [\varepsilon (\rho_l s_l \mathbf{D}_l \nabla C_l + \rho_g s_g \mathbf{D}_g \nabla C_g - \rho \mathbf{D} \nabla C)] - \nabla \cdot [(C_l - C_g) \mathbf{j}_l], \end{aligned} \tag{67}$$

conservation of energy

$$\begin{aligned} \frac{\partial}{\partial t} [(1-\varepsilon)\rho_s h_s + \varepsilon \rho h] + \nabla \cdot (\gamma_h \rho \mathbf{u} h) &= \nabla \cdot \left(\frac{k_{eff}}{c_l} \nabla h \right) \\ &+ \nabla \cdot \left[\frac{k_{eff}}{c_l} \nabla (h_l - h) \right] - \nabla \cdot [(h_l - h_g) \mathbf{j}_l] + q. \end{aligned} \tag{68}$$

In the above, the energy conservation equation can be omitted in the case of isothermal condition. The species transport equation is applicable to gas as well as liquid. Usually, C denotes the mass concentration of the more volatile component (gas), then from (36) follows that the mass concentration of liquid is $1 - C$.

The liquid diffusive mass flux $\mathbf{j}_l$ from (48) reduce to:

$$\mathbf{j}_l = \frac{\mathbf{K} \lambda_l \lambda_g}{\nu} \nabla p_c + \frac{\mathbf{K} \lambda_l \lambda_g}{\nu} (\rho_l - \rho_g) \mathbf{g}. \tag{69}$$

To close the system of conservation equations, an equilibrium phase diagram is needed. Inside the two-phase zone, thermodynamic equilibrium is assumed to hold true, and thus the concentrations of noncondensable gas in liquid and gas phases are given by their equilibrium values:

$$C_l^e = 0 \quad \text{and} \quad C_g^e = C_g^e(T, p_g). \tag{70}$$

To obtain expression for C_g^e, the assumption is used that the gas phase is an ideal mixture. First, we use the ideal gas law to obtain the densities of liquid's vapor and noncondensable gas in the gas phase:

$$\rho_v = \frac{p_v M_v}{RT}, \quad \rho_{ng} = \frac{(p_g - p_v) M_{ng}}{RT}, \tag{71}$$

where the Dalton law $p_g = p_{ng} + p_v$ was used to express the noncondensable gas pressure p_{ng} through gas phase pressure p_g and saturated vapor pressure p_v, and M_v and M_{ng} are molecular weights of vapor (liquid) and noncondensable gas.

Using the expressions (71), we obtain the gas phase density ρ_g and the equilibrium value of mass concentration C_g^e, respectively, as

$$\rho_g = \rho_v + \rho_{ng} = \frac{p_v M_v + (p_g - p_v) M_{ng}}{RT}, \tag{72}$$

$$C_g^e = \frac{\rho_{ng}}{\rho_g} = \frac{(p_g - p_v) M_{ng}}{p_v M_v + (p_g - p_v) M_{ng}} = 1 - \frac{p_v M_v}{R \rho_g T}. \tag{73}$$

Now we describe the step 3 of iterative solution procedure in section 4.3. The value of C computed from equation (67) is compared with C_l^e and C_g^e.

1. If $C \leq C_l^e$, then in this point there is only liquid phase, so that $s_l = 1$, $s_g = 0$, $C_l = C$ (in our case $C_l^e = 0$, so $C_l = 0$), $C_g = 0$.
2. If $C \geq C_g^e$, then in this point only gas phase is present, so that $s_l = 0$, $s_g = 1$, $C_l = 0$, $C_g = C$.
3. If $C_l^e \leq C \leq C_g^e$, then the point is in two-phase zone. Using the definitions (34) and (32) and the made assumption, that $C_l = C_l^e$ and $C_g = C_g^e$, we obtain the liquid saturation via the following relation:

$$s_l = \frac{\rho_g \left(C - C_g^e\right)}{\rho_l \left(C_l^e - C\right) + \rho_g \left(C - C_g^e\right)}. \tag{74}$$

According to the iterative solution procedure, obtained values are substituted back into equations, the property coefficients are updated (step 4) and so on.

4.5 MMM based two-phase model

In this subsection, following [19], a two-phase model is derived, which is based on MMM definitions of mixture properties and characteristics. For this particular model, later in this work, we develop a numerical solution algorithm and build a computer simulator. They are presented in sections 6 and 7, respectively.

First, substitution of momentum conservation equation from subsection 4.2

$$\rho \mathbf{u} = -\frac{\mathbf{K}}{\nu}\left[\nabla p - \left(\lambda_1 \rho_1 + \lambda_2 \rho_2\right) \mathbf{g}\right] \tag{75}$$

into mass conservation equation (42) for two-phase mixture yields

$$\varepsilon \frac{\partial \rho}{\partial t} - \nabla \cdot \left(\frac{\mathbf{K}}{\nu}\left[\nabla p - \left(\lambda_1 \rho_1 + \lambda_2 \rho_2\right) \mathbf{g}\right]\right) = \bar{m}, \tag{76}$$

where $\bar{m} = \bar{m}_1 + \bar{m}_2$ is the mixture mass source or sink. In the absence of any external mass source or sink, $\bar{m} = 0$.

Obtained equation is usually called pressure equation and is used to find mixture pressure p. The mixture kinematic viscosity ν is positive (see (37)). Thus if the absolute permeability tensor $\mathbf{K}$ of porous medium is positive-definite, so is $\mathbf{K}/\nu$. Consequently, it follows from (76) that the pressure equation is elliptic.

In the case of compressible flow, the first term on the left-hand side of (76) is sometimes expressed using phases compressibility coefficients c_1 and c_2:

$$\frac{\partial \rho}{\partial t} = \left(\rho_1 s_1 c_1 + \rho_2 s_2 c_2\right) \frac{\partial p}{\partial t} + \left(\rho_1 - \rho_2\right) \frac{\partial s_1}{\partial t}.$$

Then the pressure equation is parabolic. However, the compressibility of fluids is typically quite small, and the pressure reaches a steady state very rapidly.

Next, we derive the transport equation for the first phase saturation s_1. Let us consider the mass conservation equation (1) for the first phase. In section 4.2, we have obtained the expression (47) for the mass flux $\rho_1 \mathbf{u}_1$ and the

expression (48) for the diffusive mass flux $\mathbf{j}_1$ of phase 1. Substitute them into equation (1) to have

$$\varepsilon \frac{\partial (\rho_1 s_1)}{\partial t} + \nabla \cdot (\rho \mathbf{u} \lambda_1) = -\nabla \cdot \left(\frac{\mathbf{K} \lambda_1 \lambda_2}{\nu} \left[\nabla p_c + (\rho_1 - \rho_2) \mathbf{g} \right] \right) + \bar{m}_1. \qquad (77)$$

This equation is usually called saturation-conservation equation. Recall that $dp_c/ds_1 < 0$ by the property of capillary pressure. Hence if $\mathbf{K}$ is positive-definite, then (77) is degenerate parabolic problem. The degeneracy is called by the fact that λ_1 and λ_2 can be zero. When the capillary forces are small, saturation-conservation equation is advection dominated; it is purely hyperbolic in the absence of these diffusive forces.

The saturation-conservation equation (77) in conjunction with the pressure equation (76) and the Darcy law (75) makes up a full system of equations for unknowns p, $\mathbf{u}$, and s_1. This system can be used to model two-phase immiscible fluid flow, when the phase compositions are of no importance and molecular diffusion and hydraulic dispersion effects can be neglected. Note that this model can be extended to the three-phase flow with the similar saturation-conservation equation for phase 2 (or 3) or to the nonisothermal problems adding the energy equation for enthalpy (59) or temperature (64).

Otherwise, this model can be further simplified for the flow of two immiscible, incompressible fluids. Using the assumptions, that ρ_1 and ρ_2 are constant and $\bar{m}_1 = \bar{m}_2 = 0$, the mass conservation equations for phase 1 and 2 reduce to

$$\varepsilon \frac{\partial s_1}{\partial t} + \nabla \cdot \mathbf{u}_1 = 0,$$
$$\varepsilon \frac{\partial s_2}{\partial t} + \nabla \cdot \mathbf{u}_2 = 0.$$

Defining the mixture velocity as

$$\mathbf{u} = \mathbf{u}_1 + \mathbf{u}_2, \qquad (78)$$

adding the above equations and using $s_1 + s_2 = 1$, the mixture's continuity equation reduces to

$$\nabla \cdot \mathbf{u} = 0. \qquad (79)$$

In 1D case, the mixture velocity u is constant and given by boundary condition.

Similarly to section 4.2, the analogs of equations and relations in section 4.2 can be obtained for this special case. For example, the momentum conservation equation for the mixture (Darcy law) is expressed as

$$\mathbf{u} = -\frac{\mathbf{K}}{\mu} \left(\nabla p - \left(\sum_k \lambda_k \rho_k \right) \mathbf{g} \right), \qquad (80)$$

where μ is the mixture's dynamic viscosity defined as

$$\mu = \left(\sum_k \frac{k_{rk}}{\mu_k} \right)^{-1},$$

and also the phase mobility is redefined as

$$\lambda_k = \frac{k_{rk}}{\mu_k} \mu, \quad \sum_k \lambda_k = 1.$$

Substitution of (80) into (79) yields an analog of pressure equation(76).

The diffusive mass flux of phase k within the multiphase mixture is defined now as

$$\mathbf{j}_k = \mathbf{u}_k - \lambda_k \mathbf{u}, \qquad \sum_k \mathbf{j}_k = 0$$

and can be expressed as

$$\mathbf{j}_k = \frac{\mathbf{K}\lambda_k}{\mu} \sum_i \lambda_i \nabla p_{c\,ik} + \frac{\mathbf{K}\lambda_k}{\mu} \sum_i \lambda_i (\rho_k - \rho_i)\mathbf{g}.$$

An analog of equation (77) is the following equation:

$$\varepsilon \frac{\partial s_1}{\partial t} + \mathbf{u} \cdot \nabla \lambda_1 = -\nabla \cdot \left(\frac{\mathbf{K}\lambda_1\lambda_2}{\mu} \left[\nabla p_c + (\rho_1 - \rho_2)\,\mathbf{g} \right] \right). \tag{81}$$

Note that in 1D case, only this equation is needed to be solved. For equation (81) with diffusive flux $\mathbf{j}_1$ without gravity term, an exact integral solution exists in 1D case, if the boundary condition for the velocity u varies inversely proportional to the square root of time [16].

Finally, for a more complete view of the hierarchy of the multiphase flow models, it is very interesting to compare the equations (77) and (81) with the well-known Richards equation of unsaturated flow theory.

5 Unsaturated Flow Theory (UFT)

In order to alleviate the analytical and numerical difficulties associated with MFM, an approximate model called the Unsaturated Flow Theory was developed and popularly used by hydrologists [18]. Applications of UFT to the other multiphase problems in porous media were also demonstrated in the literature [15]. In this section, we briefly derive from MFM the well-known Richards equation of UFT to gain insight into the important assumptions made in the theory and thus identify its limitations in certain situations.

Substituting equation (4) into equation (1) for a liquid phase (e.g., water in hydrology), we obtain

$$\varepsilon \frac{\partial (\rho_l s_l)}{\partial t} + \nabla \cdot \left(-\mathbf{K} \frac{k_{rl}}{\nu_l} \nabla p_l + \mathbf{K} \frac{k_{rl}}{\nu_l} \rho_l \mathbf{g} \right) = \bar{m}_l. \tag{82}$$

This provides the single equation for two unknowns, s_l and p_l. To close the model, it is traditionally assumed in UFT that the gas phase (e.g., air in hydrology) essentially remains at the constant pressure (e.g., equal to atmospheric pressure):

$$p_g = const.$$

From the capillary pressure definition (5), it follows then that ∇p_l is simply given by

$$\nabla p_l = \nabla p_g - \nabla p_c = -\frac{dp_c}{ds_l} \nabla s_l. \tag{83}$$

Using equation (83) and neglecting the interphase mass transfer $\bar{m}_l$, we obtain from equation (82) the well-known Richards equation:

$$\varepsilon \frac{\partial (\rho_l s_l)}{\partial t} = \nabla \cdot (\mathbf{D} \nabla s_l) - \nabla \cdot \left(\mathbf{K} \frac{k_{rl}}{\nu_l} \rho_l \mathbf{g} \right), \tag{84}$$

where the diffusion coefficient is defined as

$$\mathbf{D}(s_l) = -\mathbf{K}\frac{k_{rl}}{\nu_l}\frac{dp_c}{ds_l}.$$

So, the limitations of UFT are that it neglects the gas phase motion, interphase mass transfer, and effects of heterogeneity on capillary pressure.

6 Numerical scheme

In this section we develop a numerical scheme for solving the two-phase model derived in subsection 4.5. First, we discuss shortly the nonlinearity and coupling of the considered differential system (76), (75), (77).

Note that coefficients of pressure equation (76) are functions of saturations, but not pressure. Therefore, according to [8], the pressure equation is weakly nonlinear. In addition, the MMM coefficient ν is a much smoother quantity than the corresponding coefficients of separate phases in MFM. Hence, the coefficients in pressure equation (76) can be explicitly treated in our numerical procedure.

In contrast, the saturation-conservation equation (77) is strongly nonlinear. The nonlinearity is caused by the phase relative permeabilities and capillary pressure. The saturation-conservation equation and the pressure equation are strongly coupled through the mixture velocity from Darcy law (75). However, in MMM with mixture pressure (sometimes also called global pressure) this coupling is much less then in the models with other pressure formulations [7].

6.1 A sequential procedure

Using the above considerations, we employ a special solution procedure to decouple our system of PDEs. It is similar to that used in [8]. We state our sequential solution procedure as follows:

1. At time moment $t = t_{i-1}$, the primary variables p and s_1 are known (from initial conditions at $t = 0$).

2. Calculate the coefficients $\nu(s_1)$, $\lambda_1(s_1)$, $\lambda_2(s_1)$, and $\rho(s_1)$ of the pressure equation (76).

3. Apply the control volume based finite difference scheme considered in subsection 6.2 to solve the pressure equation (76) for p.

4. Calculate the mixture velocity $\mathbf{u}$ from the Darcy law (75) using the same discretization scheme as in step 3, coefficients from step 2, and just obtained mixture pressure p from step 3.

5. Utilize the Picard or Newton iterations considered in subsection 6.3 to solve the saturation-conservation equation (77) for saturation s_1 with $\mathbf{u}$ from step 4.

6. Update the coefficients in step 2 and perform a few iterations (steps 2-6) at the current time level until convergence is achieved (residual of the mixture mass balance equation (76) is small enough).

7. Go to the next time step and repeat the above procedure until a final state $t = T$ is reached.

In conventional IMPES solution procedures for the simulation of multiphase flow in porous media [10], the pressure equation is solved implicitly with its coefficients evaluated explicitly, and the concentration-saturation-conservation equations (transport system) are solved explicitly. Hence, for difficult nonlinearities, IMPES methods are often forced to use extremely small time steps to stabilize the overall procedure. This leads to significantly compromised computational efficiency.

In our sequential solution procedure, the pressure and saturation-conservation equations are first decoupled, linearized, and then solved implicitly. Such procedure is sometimes also called a sequential semi-implicit method. It fully utilizes the physics of the flow and transport processes and relaxes the time step restrictions. It can also be extended in the natural way, if the model is extended with additional PDEs for saturations, concentrations or temperature.

Finally, we mention that there were attempts [39] to solve multiphase models with fully coupled and fully implicit methods. In such methods, all coupled nonlinear PDEs are simultaneously solved in an implicit fashion. Therefore, such schemes are stable for the large time steps. However, they are computationally very expensive per time step, and their application is restricted to very small problems due to the limited computational resources.

6.2 Finite difference scheme for pressure equation

For the multiphase flow models, desirable properties of the numerical method besides stability and convergence include the conservation of mass, the monotonicity of the solution (of the homogeneous equations) to avoid the nonphysical oscillations, the positive-definite matrix.

In this work, we use a cell-centered non-uniform staggered Cartesian grid to partition the problem domain Ω into the control volumes and a control volume based finite difference schemes to numerically approximate PDEs. Integrating the pressure equation (76) over the control volume V and applying the divergence theorem, we obtain

$$\int_V \varepsilon \frac{\partial \rho}{\partial t} d\mathbf{x} - \oint_{\partial V} \frac{\mathbf{K}}{\nu} \left[\nabla p - (\lambda_1 \rho_1 + \lambda_2 \rho_2)\, \mathbf{g}\right] \cdot \mathbf{n} ds = \int_V \bar{m} d\mathbf{x}.$$

In this way, the mass is conserved locally (volume by volume). Approximating full flux on the control volume interfaces, we use harmonic, arithmetic means or upstream weightings of coefficients. Obtained matrices are 3-diagonal in 1D case, 5-diagonal in 2D, and 7-diagonal in 3D. Dirichlet, Neumann, and full flux boundary conditions are implemented for all boundaries of the problem domain Ω.

6.3 Finite difference scheme for saturation-conservation equation

Similarly, from the saturation-conservation equation (77) we obtain

$$\int_V \varepsilon \frac{\partial (\rho_1 s_1)}{\partial t} d\mathbf{x} + \oint_{\partial V} \left\{ \lambda_1 \rho \mathbf{u} + \frac{\mathbf{K} \lambda_1 \lambda_2}{\nu} \left[\nabla p_c + (\rho_1 - \rho_2)\mathbf{g}\right] \right\} \cdot \mathbf{n} ds = \int_V \bar{m}_1 d\mathbf{x}.$$

To deal with the strong nonlinearity of this equation, we perform in step 5 of our sequential procedure several Picard or Newton iterations. Here is the linearization of the full flux with the Picard method:

$$\lambda_1(s_1^k)\left[(\rho_1-\rho_2)s_1^{k+1}+\rho_2\right]\mathbf{u}+\frac{\mathbf{K}\lambda_1(s_1^k)\lambda_2(s_1^k)}{\nu(s_1^k)}\left[p_c'(s_1^k)\nabla s_1^{k+1}+(\rho_1-\rho_2)\mathbf{g}\right],$$

where s_1^k and s_1^{k+1} are values from previous and current iterations, respectively. Accordingly, for the Newton iterations we use the following linearization:

$$\begin{aligned}&\left(\lambda_1(s_1^k)+\lambda_1'(s_1^k)\triangle s\right)\rho(s_1^k)\mathbf{u}\\&\quad+\frac{\mathbf{K}\lambda_1(s_1^k)\lambda_2(s_1^k)}{\nu(s_1^k)}\left[\nabla\left(p_c(s_1^k)+p_c'(s_1^k)\triangle s\right)+(\rho_1-\rho_2)\mathbf{g}\right],\end{aligned}$$

where $\triangle s = s_1^{k+1}-s_1^k$. Newton iterations generally give better convergence performance if the initial guess is good, but the Picard method is often more robust, i.e. less dependent on the initial guess.

In our control volume based finite difference scheme for saturation-conservation equation, we use the upwind discretization of the convection term with the mixture velocity $\mathbf{u}$ and the harmonic, arithmetic means or upstream weightings of coefficients approximating the diffusive flux $\mathbf{j}_1$ on the control volume interfaces. Obtained matrices are 3-diagonal in 1D case, 5-diagonal in 2D, and 7-diagonal in 3D. Dirichlet, Neumann, and full flux boundary conditions are implemented for all boundaries of the problem domain Ω.

7 Computer simulator

In this section, we present a computer simulator for the two-phase immiscible flow in porous media, which solves the differential model from the subsection 4.5 using the numerical scheme described in the previous section.

Like it becomes recently more and more popular in the scientific computing, we exploit the object-oriented programming (OOP) techniques in the design and implementation of our simulation code. This allows to reduce the amount of time spent on the programming and debugging and makes all implementational aspects cleaner and simpler.

According to the strategy proposed in [13] and used in Diffpack software library, we build our simulator for the system of PDEs by merging together independent solvers for alone-standing equations that enter the system. Therefore, first we create a solver for the pressure equation (76) and debug it for a simple coefficients: constants or known spatial functions, for which we can find analytical solutions. This solver class is shown in Figure 2 as Pressure. Similarly, we develop and debug a solver class Saturation for the saturation-conservation equation (77).

The equations become coupled into the system through the coefficients. In our PDE solvers, these coefficients, including the source, initial and boundary conditions functions, are represented by virtual functions. Subclasses of PDE solvers override these functions and implement the physically relevant versions, when the coefficients are coupled to other unknown fields in the PDE system. All these functions are often built of a common set of relations (constitutive relationships, MMM definitions etc.). Therefore, they are collected in class

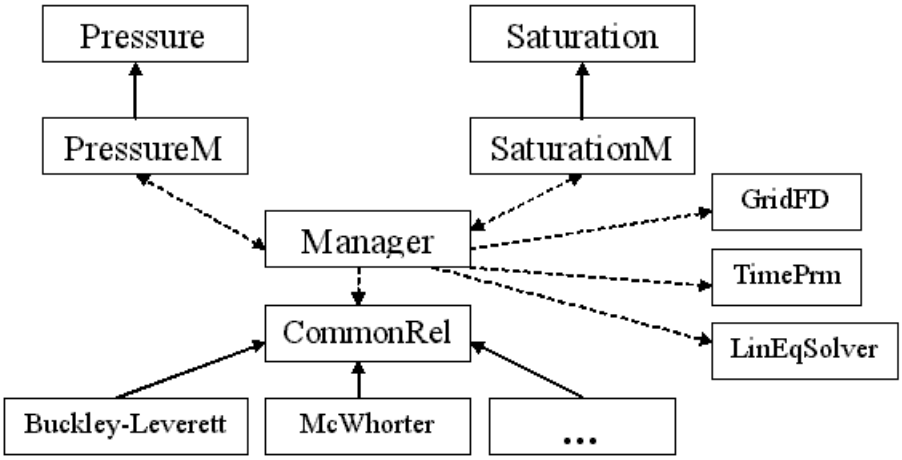

Figure 2: Design of the PDE system solver with relations between solver classes, manager and pool of common relations. Solid arrows indicate inheritance ("is-a" relationship, with arrows pointing from subclass to base class). Dashed arrows indicate pointer ("has-a" relationship).

hierarchies and accessed from PDE solvers through a base class CommonRel interface (pointer). Note that constitutive relationships can be easily changed without affecting the code in PDE solvers.

A manage class, called Manager, acts as the solver class for the whole PDE system. This class contains two-way pointers to the subclasses for solving the pressure and saturation-conservation equations - PressureM and SaturationM, respectively, which enable the coupling by overriding the virtual functions of base classes with the functions from common relation hierarchy. The manager is also responsible for creating a space grid and time discretization. It allocates a common linear system and solver object, and distributes all these data to the PDE solver classes.

Finally, we note that such design of PDE system solver suits very well to the sequential solution procedure, which was chosen to decouple the system in subsection 6.1. It is likewise naturally extensible if the differential model is extended with the additional PDEs according to the subsection 4.5.

8 Numerical tests

8.1 Multiphase flow without capillary pressure effects - Buckley-Leverett problem 1D

A standard method for the verification of multiphase flow models for processes without capillary pressure effects is Buckley-Leverett problem. It describes the unsteady displacement of oil by water in one-dimensional system, when externally applied driving forces are large in relation to the gradient of capillary pressure. This problem has analytical solution [10, 16].

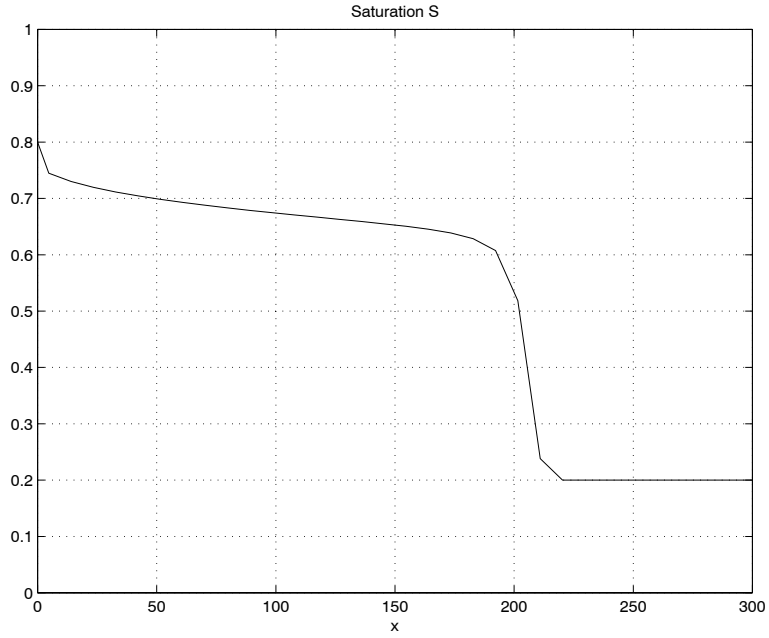

Figure 3: Buckley-Leverett problem 1D

Figure 3 shows the numerical results obtained with the data from [10]. This is the saturation distribution of infiltrating water phase after a period of 1500 days. The initial water saturation was 0.2 everywhere. Water is injected at rate $1.5 \cdot 10^{-4}$ $[kg/(m^2 s]$ at the left boundary, where the water saturation is 0.8. Brooks and Corey expressions (23) for relative permeabilities are used.

As one can see, our numerical scheme shows a monotonic solution behavior, i.e. no non-physical oscillations occur. Mass conservation and front velocity are approximated in a physically correct way. However, from the upwind method, that we are using, is resulting the artificial diffusion. It is leading to a smearing of the saturation front.

Since the nonlinear convective equation is self-sharpening, the effects of artificial diffusion are of less importance for nonlinear systems than for linear systems. However, application of an upwind method of higher order is needed to increase the convergence velocity and thus improve the front.

8.2 Multiphase flow with capillary pressure effects - McWhorter problem

McWhorter and Sunada [16] have derived an exact integral solutions for the horizontal (one-dimensional), unsteady flow of two viscous, incompressible fluids with full consideration of capillary drive and for arbitrary capillary pressure and relative permeability functions. Therefore, McWhorter problem is often used for testing on two-phase processes with capillary forces.

Figure 4 shows the numerical results obtained for one-dimensional, unidirectional displacement of a nonwetting phase by entry of a wetting phase (see [16]). The flux q_w of wetting phase through the left boundary is proportional

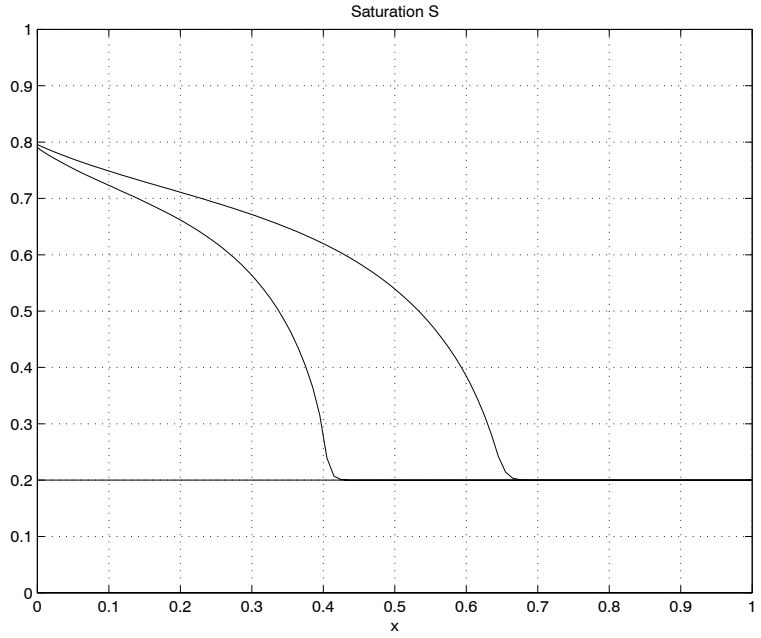

Figure 4: McWhorter problem 1D

to $t^{-1/2}$. The initial water saturation was 0.2 everywhere. Brooks and Corey expressions (23) for relative permeabilities are used.

Analyzing the shape of saturation profiles for two selected time moments, influence of the diffusive capillary forces can be clearly seen.

8.3 Multiphase flow with heterogeneous effects - Buckley-Leverett problem 2D

This 2D problem has a simple heterogeneity. Inside the rectangular $[0.3, 0.7] \times [0.3, 0.7]$ the absolute permeability is 0.01, while outside, the absolute permeability is 0.1. This is actually a very mild form of the heterogeneity, compared to those encountered in the modeling of waste cover systems.

Similarly to 1D case, the water was injected at the bottom. Figure 5 shows the numerical results: isolines of water saturation and velocity of the oil.

Acknowledgements. The author is thankful to the Research and Training Network on "Hyperbolic and Kinetic Equations" for the financial support for his stay in the Fraunhofer ITWM, Kaiserlsuatern. The creative collaboration with colleagues from the Fraunhofer ITWM (Dr.Steiner, Dr.Iliev, Dr.Linn, and many others), their hospitality and the friendly atmosphere there are highly appreciated.

References

[1] L. M. Abriola and G. F. Pinder, A multiphase approach to the modeling of porous media contamination by organic compounds 1. Equation devel-

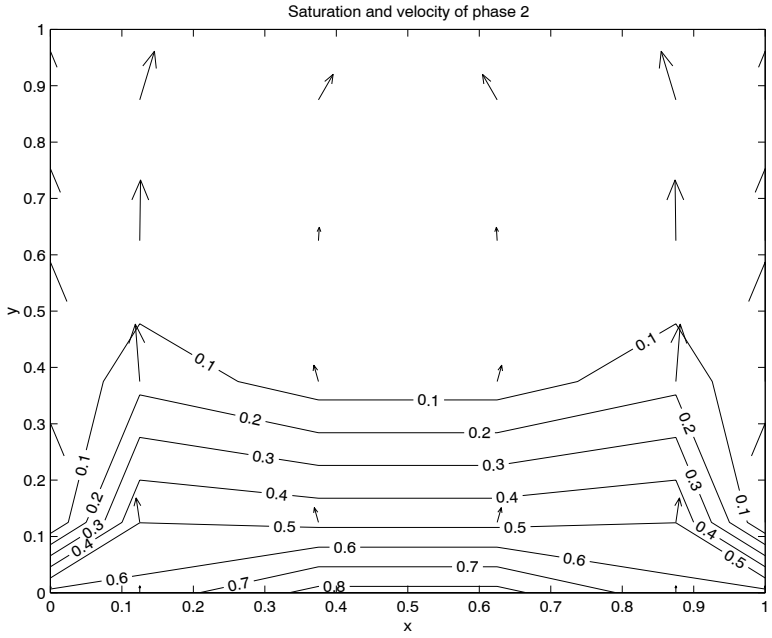

Figure 5: Buckley-Leverett problem 2D

opment. *Water Resour. Res.*, **21**, 11–18 (1985).

[2] L. M. Abriola, *Multiphase Flow and Transport Models for Organic Chemicalls: A Review and Assessment.* EA-5976, EPRI Palo Alto, CA, 1988.

[3] M. B. Allen III, Numerical modeling of multiphase flow in porous media. *Adv. Water Resour.*, **9**, 162–187 (1985).

[4] J. Bear, *Dynamics of Fluids in Porous Media.* Elsevier, New York (1972).

[5] P. Cheng, Heat transfer in geothermal systems. *Advances in Heat Transfer*, **14**, 1–105 (1978).

[6] Z. Chen and R. Ewing, Fully discrete finite element analysis of multiphase flow in groundwater hydrology. *SIAM J. Numer. Anal.*, **34**, 2228–2253 (1997).

[7] Z. Chen and R. E. Ewing, Comparison of various formulations of three-phase flow in porous media. *Journal of Computational Physics*, **132**, 362–373 (1997).

[8] Z. Chen, G. Qin, and R. E. Ewing, Analysis of compositional model for fluid flow in porous media. *SIAM J. APPL. MATH.*, **60**, No. 3, 747–777 (2000).

[9] R. E. Ewing and H. Wang, A summary of numerical methods for time-dependent advection-dominated partial differential equations. *Journal of Computational and Applied Mathematics*, **128**, 423–445 (2001).

[10] R. Helmig, *Multiphase Flow and Transport Processes in Subsurface: A Contribution to the Modeling of Hydrosystems*. Springler Verlag, Berlin (1997).

[11] W. Jäger and J. Kačur, Solution of porous medium systems by linear approximation scheme. *Numer. Math.*, **60**, 407–427 (1991).

[12] M. Kaviany, *Principles of Heat Transfer in Porous Media*. Springler-Verlag, Berlin (1991).

[13] H. P. Langtangen and O. Munthe, Solving systems of partial differential equations using object-oriented programming techniques with coupled heat and fluid flow as example. *ACM Transactions on mathematical software*, **27**, No. 1, 1-26 (2001).

[14] W. Liu, S. W. Peng, and K. Mizukami, A general mathematical modelling for heat and mass transfer in unsaturated porous media: an application to free evaporative cooling. *Heat and Mass Transfer*, **31**, 49–55 (1995).

[15] A. Majumdar and C. L. Tien, Effects of surface tension on film condensation using porous fins. *J. Heat Transfer*, **112**, 751–757 (1990).

[16] D. B. McWhorter and D. K. Sunada, Exact integral solutions for two-phase flow. *Water Resour. Res.*, **26**, 399–414 (1990).

[17] J. Molenaar, Nonlinear multigrid for fully-implicit and high-order accurate simulation of multiphase flow in porous media. *CWI Report MAS-R9712*, 1997.

[18] H. J. Morel-Seytoux, Two-phase flow in porous media. *Adv. Hydrosci.*, **9**, 119–202 (1973).

[19] C. Y. Wang and P. Cheng, Multiphase flow and heat transfer in porous media. *Advances in Heat Transfer*, **30**, 93–196 (1997).

[20] C. Y. Wang and P. Cheng, A multiphase mixture model for multiphase, multicomponent transport in capillary porous media. Part I: Model development. *Int. J. Heat Mass Transfer*, **39**, 3607–3618 (1996).

[21] P. Cheng and C. Y. Wang, A multiphase mixture model for multiphase, multicomponent transport in capillary porous media. Part II: Numerical simulation of the transport of organic compounds in the subsurface. *Int. J. Heat Mass Transfer*, **39**, 3619–3632 (1996).

[22] A. Mhimid, Theoreical study of heat and mass transfer in a zeolite bed during water desorption: validity of local thermal equilibrium assumption. *Int. J. Heat Mass Transfer*, **41**, 2967–2977 (1998).

[23] S. Whitaker, Improved constraints for the principle of local thermal equilibrium. *Ind. Eng. Chem. Res.*, **30**, 983–997 (1991).

[24] S. Whitaker, Simultaneous heat, mass, and momentum transfer in porous media: A theory of drying. In *Advances in Heat Transfer*, **13**, 119–203 (1977).

[25] A. Amiri and K. Vafai, Analysis of dispersion effects and non-thermal equilibrium, non-Darcian, variable porosity incompressible flow through porous media. *Int. J. Heat Mass Transfer*, **37**, 939–954 (1994).

[26] J. C. Parker, Multiphase flow and transport in porous media. *Rev. Geophys.*, **27**, 311–328 (1989).

[27] M. C. Leverett, Capillary behavior in porous media. *AIME Trans.*, **142**, 152–169 (1941).

[28] K. S. Udell, Heat transfer in porous media considering phase change and capillarity - the heat pipe effect. *Int. J. Heat Mass Transfer*, **28**, 485–495 (1985).

[29] K. Grosser, R. G. Carbonell, and S. Sundaresan, Onset of pulsing in two-phase cocurrent downflow through a packed bed. *A. I. Ch. E. Jl*, **34**, 1850–1860 (1988).

[30] M. Th. van Genuchten, A closed form equation for predicting the hydraulic conductivity of unsaturated soils. *Soil Science Society*, **44**, 892–898 (1980).

[31] R. H. Brooks and A. T. Corey, Hydraulic properties of porous media. *Hydrol. Pap.*, **3** (1964).

[32] J. C. Parker, R. J. Lenhard, and T. Kuppusamy, A parametric model for constitutive properties governing multiphase flow in porous media. *Water Resour. Res.*, **23**, 618–624 (1987).

[33] C. H. Sondergeld and D. L. Turcotte, An experimental study for two-phase convection in a porous medium with application to geological problems. *J. Geophys. Res.*, **82**, 2045–2053 (1977).

[34] M. R. J. Wyllie, Relative permeability. In *Petroleum Production Handbook* (Edited by T.C. Frick), Chap. 25, McGraw-Hill, New York (1962).

[35] P. M. Adler,*Porous Media, Geometry and Transports*. Butterworth-Heinemann, Boston (1992).

[36] J. M. Hernandez and J. R. Puiggali, Simulation of drying of coniferous wood using various processes. *International Chemical Engineering*, **34**, No. 3, 339–350 (1994).

[37] H. Brenner and D. A. Edwards,*Macrotransport Processes*. Butterworth-Heinemann, Boston (1993).

[38] D. L. Koch and J. Brady, Dispersion in fixed beds. *J. Fluid Mech.*, **154**, 399–427 (1985).

[39] T. F. Russell and M. F. Wheeler, Finite element and finite difference methods for continuous flows in porous media. *The Mathematics of Reservoir Simulation* (R.E. Ewing, ed.), *Frontiers in Applied Mathematics* **1**, *SIAM*, Philadelphia, 35–106 (1983).

[40] M. D. Wilkins, L. M. Abriola, and K. D. Pennnell, An experimental investigation of rate-limited nonaqueous phase liquid volatilization in unsaturated porous media: Steady state mass transfer. *Water Resour. Res.*, **31**, 2159 (1995).

[41] M. Quintard and S. Whitaker, Convection, dispersion, and interfacial transport of contaminants: homogeneous porous media. *Adv. Water Resour.*, **17**, 221–239 (1994).

[42] A. A. Baker, L. W. Gelhar, A. L. Gutjahr, J. R. Macmillan, Stochastic analysis of spatial variability in subsurface flows, I. Comparison of one- and three-dimensional flows. *Water Resour. Res.*, **14**, 263–271 (1978).

[43] G. Dagan,*Flow and Transport in Porous Formations.* Springer-Verlag, Berlin-Heidelberg (1989).

[44] Wu-Shung-Fu and Hsin-Chien-Huang, Effects of a random porosity model on heat transfer performance of porous media. *Int. J. Heat Mass Transfer*, **42**, 13–25 (1999).

[45] G. E. Mueller, Prediction of radial porosity distribution in randomly packed fixed beds of uniformly sized spheres in cylindrical containers. *Chem. Engng Sci.*, **46**, 706–708 (1991).

[46] Y. K. Chuah and V. P. Carey, Analysis of boiling heat transfer and two-phase flow in porous media with non-uniform porosity. *Int. J. Heat Mass Transfer*, **28**, 147–154 (1985).

[47] D. A. Nield and A. Bejan,*Convection in porous media.* Springer-Verlag, New York (1992).

[48] A. K. Stubos, C. Satik, and Y. C. Yortsos, Effects of capillary heterogeneity on vapor-liquid counterflow in porous media. *Int. J. Heat Mass Transfer*, **36**, 967–976 (1993).

[49] Y. C. Yortsos and J. Chang, Capillary effects on steady state flow in heterogeneous cores. *Transp. Porous Media*, **5**, 399–420 (1990).

[50] L. Gu, M. V. Swami, and P. Fairey, Generalized theoretical model of combined heat, air and moisture transfer in porous media. In*Multiphase Transport in Porous Media*, ASME HTD-Vol.**265**, 47–55 (1993).

[51] C. Satik, M. Parlar, and Y. C. Yortsos, A study of steady-state steam-water counterflow in porous media. *Int. J. Heat Mass Transfer*, **34**, 1755–1772 (1991).

[52] K. S. Udell and J. S. Fitch, Heat and mass transfer in capillary porous media considering evaporation, condensation and non-condensable gas effects. In*Heat Transfer in Porous Media and Particulate Flows*, ASME HTD-Vol. **46**, 103–110 (1985).

[53] G. Chavent, A new formulation of diphasic incompressible flow in porous media. *Lecture Notes in Mathematics*, **503**, (1976).

[54] Z. H. Wang, C. Y. Wang, and K. S. Chen, Two-phase flow and transport in the air cathode of proton exchange membrane fuel cells. *Journal of Power Sources*, **4094**, 1–11 (2000).

[55] C. Y. Wang, A fixed-grid numerical algorithm for two-phase flow and heat transfer in porous media. *Numerical Heat Transfer, Part B*, **31**, 85–105 (1997).

[56] T. S. Zhao, P. Cheng, and C. Y. Wang, Buoyancy-induced flows and phase-change heat transfer in a vertical capillary structure with symmetric heating. *Chemical Engineering Science*, **55**, 2653–2661 (2000).

[57] Y. T. Shah, *Gas-Liquid-Solid Reactor Design*. McGraw-Hill, New York, 1979.

[58] T. Boberg, *Thermal Methods of Oil Recovery*. Wiley, New York, 1988.

[59] V. K. Dhir, Boiling and two-phase flow in porous media. *Annu. Rev. Heat Transfer*, **5**, 303–350 (1994).

[60] C. Doughty and K. Pruess, A semianalytical solution for heat-pipe effects near high-level nuclear waste packages buried in partially saturated geological media. *Int. J. Heat Mass Transfer*, **31**, 79–90 (1988).

[61] K. Hiltunen, *Mathematical and numerical modeling of consolidation processes in paper machines*. PhD thesis, University of Jyväskylä, Departament of Mathematics, 1995.

[62] S. Patankar, *Numerical Heat Transfer and Fluid Flow*. Hemisphere, New-York (1980).

Published reports of the Fraunhofer ITWM

The PDF-files of the following reports are available under:
www.itwm.fraunhofer.de/rd/presse/berichte

1. D. Hietel, K. Steiner, J. Struckmeier

A Finite - Volume Particle Method for Compressible Flows

We derive a new class of particle methods for conservation laws, which are based on numerical flux functions to model the interactions between moving particles. The derivation is similar to that of classical Finite-Volume methods; except that the fixed grid structure in the Finite-Volume method is substituted by so-called mass packets of particles. We give some numerical results on a shock wave solution for Burgers equation as well as the well-known one-dimensional shock tube problem.
(19 pages, 1998)

2. M. Feldmann, S. Seibold

Damage Diagnosis of Rotors: Application of Hilbert Transform and Multi-Hypothesis Testing

In this paper, a combined approach to damage diagnosis of rotors is proposed. The intention is to employ signal-based as well as model-based procedures for an improved detection of size and location of the damage. In a first step, Hilbert transform signal processing techniques allow for a computation of the signal envelope and the instantaneous frequency, so that various types of non-linearities due to a damage may be identified and classified based on measured response data. In a second step, a multi-hypothesis bank of Kalman Filters is employed for the detection of the size and location of the damage based on the information of the type of damage provided by the results of the Hilbert transform.
Keywords: Hilbert transform, damage diagnosis, Kalman filtering, non-linear dynamics
(23 pages, 1998)

3. Y. Ben-Haim, S. Seibold

Robust Reliability of Diagnostic Multi-Hypothesis Algorithms: Application to Rotating Machinery

Damage diagnosis based on a bank of Kalman filters, each one conditioned on a specific hypothesized system condition, is a well recognized and powerful diagnostic tool. This multi-hypothesis approach can be applied to a wide range of damage conditions. In this paper, we will focus on the diagnosis of cracks in rotating machinery. The question we address is: how to optimize the multi-hypothesis algorithm with respect to the uncertainty of the spatial form and location of cracks and their resulting dynamic effects. First, we formulate a measure of the reliability of the diagnostic algorithm, and then we discuss modifications of the diagnostic algorithm for the maximization of the reliability. The reliability of a diagnostic algorithm is measured by the amount of uncertainty consistent with no-failure of the diagnosis. Uncertainty is quantitatively represented with convex models.
Keywords: Robust reliability, convex models, Kalman filtering, multi-hypothesis diagnosis, rotating machinery, crack diagnosis
(24 pages, 1998)

4. F.-Th. Lentes, N. Siedow

Three-dimensional Radiative Heat Transfer in Glass Cooling Processes

For the numerical simulation of 3D radiative heat transfer in glasses and glass melts, practically applicable mathematical methods are needed to handle such problems optimal using workstation class computers. Since the exact solution would require super-computer capabilities we concentrate on approximate solutions with a high degree of accuracy. The following approaches are studied: 3D diffusion approximations and 3D ray-tracing methods.
(23 pages, 1998)

5. A. Klar, R. Wegener

A hierarchy of models for multilane vehicular traffic
Part I: Modeling

In the present paper multilane models for vehicular traffic are considered. A microscopic multilane model based on reaction thresholds is developed. Based on this model an Enskog like kinetic model is developed. In particular, care is taken to incorporate the correlations between the vehicles. From the kinetic model a fluid dynamic model is derived. The macroscopic coefficients are deduced from the underlying kinetic model. Numerical simulations are presented for all three levels of description in [10]. Moreover, a comparison of the results is given there.
(23 pages, 1998)

Part II: Numerical and stochastic investigations

In this paper the work presented in [6] is continued. The present paper contains detailed numerical investigations of the models developed there. A numerical method to treat the kinetic equations obtained in [6] are presented and results of the simulations are shown. Moreover, the stochastic correlation model used in [6] is described and investigated in more detail.
(17 pages, 1998)

6. A. Klar, N. Siedow

Boundary Layers and Domain Decomposition for Radiative Heat Transfer and Diffusion Equations: Applications to Glass Manufacturing Processes

In this paper domain decomposition methods for radiative transfer problems including conductive heat transfer are treated. The paper focuses on semi-transparent materials, like glass, and the associated conditions at the interface between the materials. Using asymptotic analysis we derive conditions for the coupling of the radiative transfer equations and a diffusion approximation. Several test cases are treated and a problem appearing in glass manufacturing processes is computed. The results clearly show the advantages of a domain decomposition approach. Accuracy equivalent to the solution of the global radiative transfer solution is achieved, whereas computation time is strongly reduced.
(24 pages, 1998)

7. I. Choquet

Heterogeneous catalysis modelling and numerical simulation in rarified gas flows Part I: Coverage locally at equilibrium

A new approach is proposed to model and simulate numerically heterogeneous catalysis in rarefied gas flows. It is developed to satisfy all together the following points:
1) describe the gas phase at the microscopic scale, as required in rarefied flows,
2) describe the wall at the macroscopic scale, to avoid prohibitive computational costs and consider not only crystalline but also amorphous surfaces,
3) reproduce on average macroscopic laws correlated with experimental results and
4) derive analytic models in a systematic and exact way. The problem is stated in the general framework of a non static flow in the vicinity of a catalytic and non porous surface (without aging). It is shown that the exact and systematic resolution method based on the Laplace transform, introduced previously by the author to model collisions in the gas phase, can be extended to the present problem. The proposed approach is applied to the modelling of the EleyRideal and LangmuirHinshelwood recombinations, assuming that the coverage is locally at equilibrium. The models are developed considering one atomic species and extended to the general case of several atomic species. Numerical calculations show that the models derived in this way reproduce with accuracy behaviors observed experimentally.
(24 pages, 1998)

8. J. Ohser, B. Steinbach, C. Lang

Efficient Texture Analysis of Binary Images

A new method of determining some characteristics of binary images is proposed based on a special linear filtering. This technique enables the estimation of the area fraction, the specific line length, and the specific integral of curvature. Furthermore, the specific length of the total projection is obtained, which gives detailed information about the texture of the image. The influence of lateral and directional resolution depending on the size of the applied filter mask is discussed in detail. The technique includes a method of increasing directional resolution for texture analysis while keeping lateral resolution as high as possible.
(17 pages, 1998)

9. J. Orlik

Homogenization for viscoelasticity of the integral type with aging and shrinkage

A multiphase composite with periodic distributed inclusions with a smooth boundary is considered in this contribution. The composite component materials are supposed to be linear viscoelastic and aging (of the nonconvolution integral type, for which the Laplace transform with respect to time is not effectively applicable) and are subjected to isotropic shrinkage. The free shrinkage deformation can be considered as a fictitious temperature deformation in the behavior law. The procedure presented in this paper proposes a way to determine average (effective homogenized) viscoelastic and shrinkage (temperature) composite properties and the homogenized stressfield from known properties of the components. This is done by the extension of the asymptotic homogenization technique known for pure elastic nonhomogeneous bodies to the nonhomogeneous thermoviscoelasticity of the integral noncon-

volution type. Up to now, the homogenization theory has not covered viscoelasticity of the integral type. SanchezPalencia (1980), Francfort & Suquet (1987) (see [2], [9]) have considered homogenization for viscoelasticity of the differential form and only up to the first derivative order. The integralmodeled viscoelasticity is more general then the differential one and includes almost all known differential models. The homogenization procedure is based on the construction of an asymptotic solution with respect to a period of the composite structure. This reduces the original problem to some auxiliary boundary value problems of elasticity and viscoelasticity on the unit periodic cell, of the same type as the original non-homogeneous problem. The existence and uniqueness results for such problems were obtained for kernels satisfying some constrain conditions. This is done by the extension of the Volterra integral operator theory to the Volterra operators with respect to the time, whose 1 kernels are space linear operators for any fixed time variables. Some ideas of such approach were proposed in [11] and [12], where the Volterra operators with kernels depending additionally on parameter were considered. This manuscript delivers results of the same nature for the case of the spaceoperator kernels.
(20 pages, 1998)

10. J. Mohring

Helmholtz Resonators with Large Aperture

The lowest resonant frequency of a cavity resonator is usually approximated by the classical Helmholtz formula. However, if the opening is rather large and the front wall is narrow this formula is no longer valid. Here we present a correction which is of third order in the ratio of the diameters of aperture and cavity. In addition to the high accuracy it allows to estimate the damping due to radiation. The result is found by applying the method of matched asymptotic expansions. The correction contains form factors describing the shapes of opening and cavity. They are computed for a number of standard geometries. Results are compared with numerical computations.
(21 pages, 1998)

11. H. W. Hamacher, A. Schöbel

On Center Cycles in Grid Graphs

Finding "good" cycles in graphs is a problem of great interest in graph theory as well as in locational analysis. We show that the center and median problems are NP hard in general graphs. This result holds both for the variable cardinality case (i.e. all cycles of the graph are considered) and the fixed cardinality case (i.e. only cycles with a given cardinality p are feasible). Hence it is of interest to investigate special cases where the problem is solvable in polynomial time. In grid graphs, the variable cardinality case is, for instance, trivially solvable if the shape of the cycle can be chosen freely. If the shape is fixed to be a rectangle one can analyze rectangles in grid graphs with, in sequence, fixed dimension, fixed cardinality, and variable cardinality. In all cases a complete characterization of the optimal cycles and closed form expressions of the optimal objective values are given, yielding polynomial time algorithms for all cases of center rectangle problems. Finally, it is shown that center cycles can be chosen as rectangles for small cardinalities such that the center cycle problem in grid graphs is in these cases completely solved.
(15 pages, 1998)

12. H. W. Hamacher, K.-H. Küfer

Inverse radiation therapy planning - a multiple objective optimisation approach

For some decades radiation therapy has been proved successful in cancer treatment. It is the major task of clinical radiation treatment planning to realize on the one hand a high level dose of radiation in the cancer tissue in order to obtain maximum tumor control. On the other hand it is obvious that it is absolutely necessary to keep in the tissue outside the tumor, particularly in organs at risk, the unavoidable radiation as low as possible.
No doubt, these two objectives of treatment planning - high level dose in the tumor, low radiation outside the tumor - have a basically contradictory nature. Therefore, it is no surprise that inverse mathematical models with dose distribution bounds tend to be infeasible in most cases. Thus, there is need for approximations compromising between overdosing the organs at risk and underdosing the target volume.
Differing from the currently used time consuming iterative approach, which measures deviation from an ideal (non-achievable) treatment plan using recursively trial-and-error weights for the organs of interest, we go a new way trying to avoid a priori weight choices and consider the treatment planning problem as a multiple objective linear programming problem: with each organ of interest, target tissue as well as organs at risk, we associate an objective function measuring the maximal deviation from the prescribed doses.
We build up a data base of relatively few efficient solutions representing and approximating the variety of Pareto solutions of the multiple objective linear programming problem. This data base can be easily scanned by physicians looking for an adequate treatment plan with the aid of an appropriate online tool.
(14 pages, 1999)

13. C. Lang, J. Ohser, R. Hilfer

On the Analysis of Spatial Binary Images

This paper deals with the characterization of microscopically heterogeneous, but macroscopically homogeneous spatial structures. A new method is presented which is strictly based on integral-geometric formulae such as Crofton's intersection formulae and Hadwiger's recursive definition of the Euler number. The corresponding algorithms have clear advantages over other techniques. As an example of application we consider the analysis of spatial digital images produced by means of Computer Assisted Tomography.
(20 pages, 1999)

14. M. Junk

On the Construction of Discrete Equilibrium Distributions for Kinetic Schemes

A general approach to the construction of discrete equilibrium distributions is presented. Such distribution functions can be used to set up Kinetic Schemes as well as Lattice Boltzmann methods. The general principles are also applied to the construction of Chapman Enskog distributions which are used in Kinetic Schemes for compressible Navier-Stokes equations.
(24 pages, 1999)

15. M. Junk, S. V. Raghurame Rao

A new discrete velocity method for Navier-Stokes equations

The relation between the Lattice Boltzmann Method, which has recently become popular, and the Kinetic Schemes, which are routinely used in Computational Fluid Dynamics, is explored. A new discrete velocity model for the numerical solution of Navier-Stokes equations for incompressible fluid flow is presented by combining both the approaches. The new scheme can be interpreted as a pseudo-compressibility method and, for a particular choice of parameters, this interpretation carries over to the Lattice Boltzmann Method.
(20 pages, 1999)

16. H. Neunzert

Mathematics as a Key to Key Technologies

The main part of this paper will consist of examples, how mathematics really helps to solve industrial problems; these examples are taken from our Institute for Industrial Mathematics, from research in the Technomathematics group at my university, but also from ECMI groups and a company called TecMath, which originated 10 years ago from my university group and has already a very successful history.
(39 pages (4 PDF-Files), 1999)

17. J. Ohser, K. Sandau

Considerations about the Estimation of the Size Distribution in Wicksell's Corpuscle Problem

Wicksell's corpuscle problem deals with the estimation of the size distribution of a population of particles, all having the same shape, using a lower dimensional sampling probe. This problem was originary formulated for particle systems occurring in life sciences but its solution is of actual and increasing interest in materials science. From a mathematical point of view, Wicksell's problem is an inverse problem where the interesting size distribution is the unknown part of a Volterra equation. The problem is often regarded ill-posed, because the structure of the integrand implies unstable numerical solutions. The accuracy of the numerical solutions is considered here using the condition number, which allows to compare different numerical methods with different (equidistant) class sizes and which indicates, as one result, that a finite section thickness of the probe reduces the numerical problems. Furthermore, the relative error of estimation is computed which can be split into two parts. One part consists of the relative discretization error that increases for increasing class size, and the second part is related to the relative statistical error which increases with decreasing class size. For both parts, upper bounds can be given and the sum of them indicates an optimal class width depending on some specific constants.
(18 pages, 1999)

18. E. Carrizosa, H. W. Hamacher, R. Klein, S. Nickel

Solving nonconvex planar location problems by finite dominating sets

It is well-known that some of the classical location problems with polyhedral gauges can be solved in polynomial time by finding a finite dominating set, i.e. a finite set of candidates guaranteed to contain at least one optimal location.
In this paper it is first established that this result holds

for a much larger class of problems than currently considered in the literature. The model for which this result can be proven includes, for instance, location problems with attraction and repulsion, and location-allocation problems.
Next, it is shown that the approximation of general gauges by polyhedral ones in the objective function of our general model can be analyzed with regard to the subsequent error in the optimal objective value. For the approximation problem two different approaches are described, the sandwich procedure and the greedy algorithm. Both of these approaches lead - for fixed epsilon - to polynomial approximation algorithms with accuracy epsilon for solving the general model considered in this paper.
Keywords: Continuous Location, Polyhedral Gauges, Finite Dominating Sets, Approximation, Sandwich Algorithm, Greedy Algorithm
(19 pages, 2000)

19. A. Becker

A Review on Image Distortion Measures

Within this paper we review image distortion measures. A distortion measure is a criterion that assigns a "quality number" to an image. We distinguish between mathematical distortion measures and those distortion measures in-cooperating a priori knowledge about the imaging devices (e. g. satellite images), image processing algorithms or the human physiology. We will consider representative examples of different kinds of distortion measures and are going to discuss them.
Keywords: Distortion measure, human visual system
(26 pages, 2000)

20. H. W. Hamacher, M. Labbé, S. Nickel, T. Sonneborn

Polyhedral Properties of the Uncapacitated Multiple Allocation Hub Location Problem

We examine the feasibility polyhedron of the uncapacitated hub location problem (UHL) with multiple allocation, which has applications in the fields of air passenger and cargo transportation, telecommunication and postal delivery services. In particular we determine the dimension and derive some classes of facets of this polyhedron. We develop some general rules about lifting facets from the uncapacitated facility location (UFL) for UHL and projecting facets from UHL to UFL. By applying these rules we get a new class of facets for UHL which dominates the inequalities in the original formulation. Thus we get a new formulation of UHL whose constraints are all facet–defining. We show its superior computational performance by benchmarking it on a well known data set.
Keywords: integer programming, hub location, facility location, valid inequalities, facets, branch and cut
(21 pages, 2000)

21. H. W. Hamacher, A. Schöbel

Design of Zone Tariff Systems in Public Transportation

Given a public transportation system represented by its stops and direct connections between stops, we consider two problems dealing with the prices for the customers: The fare problem in which subsets of stops are already aggregated to zones and "good" tariffs have to be found in the existing zone system. Closed form solutions for the fare problem are presented for three objective functions. In the zone problem the design of the zones is part of the problem. This problem is NP hard and we therefore propose three heuristics which prove to be very successful in the redesign of one of Germany's transportation systems.
(30 pages, 2001)

22. D. Hietel, M. Junk, R. Keck, D. Teleaga:

The Finite-Volume-Particle Method for Conservation Laws

In the Finite-Volume-Particle Method (FVPM), the weak formulation of a hyperbolic conservation law is discretized by restricting it to a discrete set of test functions. In contrast to the usual Finite-Volume approach, the test functions are not taken as characteristic functions of the control volumes in a spatial grid, but are chosen from a partition of unity with smooth and overlapping partition functions (the particles), which can even move along pre- scribed velocity fields. The information exchange between particles is based on standard numerical flux functions. Geometrical information, similar to the surface area of the cell faces in the Finite-Volume Method and the corresponding normal directions are given as integral quantities of the partition functions. After a brief derivation of the Finite-Volume-Particle Method, this work focuses on the role of the geometric coefficients in the scheme.
(16 pages, 2001)

23. T. Bender, H. Hennes, J. Kalcsics, M. T. Melo, S. Nickel

Location Software and Interface with GIS and Supply Chain Management

The objective of this paper is to bridge the gap between location theory and practice. To meet this objective focus is given to the development of software capable of addressing the different needs of a wide group of users. There is a very active community on location theory encompassing many research fields such as operations research, computer science, mathematics, engineering, geography, economics and marketing. As a result, people working on facility location problems have a very diverse background and also different needs regarding the software to solve these problems. For those interested in non-commercial applications (e. g. students and researchers), the library of location algorithms (LoLA can be of considerable assistance. LoLA contains a collection of efficient algorithms for solving planar, network and discrete facility location problems. In this paper, a detailed description of the functionality of LoLA is presented. In the fields of geography and marketing, for instance, solving facility location problems requires using large amounts of demographic data. Hence, members of these groups (e. g. urban planners and sales managers) often work with geographical information too s. To address the specific needs of these users, LoLA was inked to a geographical information system (GIS) and the details of the combined functionality are described in the paper. Finally, there is a wide group of practitioners who need to solve large problems and require special purpose software with a good data interface. Many of such users can be found, for example, in the area of supply chain management (SCM). Logistics activities involved in strategic SCM include, among others, facility location planning. In this paper, the development of a commercial location software tool is also described. The too is embedded in the Advanced Planner and Optimizer SCM software developed by SAP AG, Walldorf, Germany. The paper ends with some conclusions and an outlook to future activities.
Keywords: facility location, software development, geographical information systems, supply chain management.
(48 pages, 2001)

24. H. W. Hamacher, S. A. Tjandra

Mathematical Modelling of Evacuation Problems: A State of Art

This paper details models and algorithms which can be applied to evacuation problems. While it concentrates on building evacuation many of the results are applicable also to regional evacuation. All models consider the time as main parameter, where the travel time between components of the building is part of the input and the overall evacuation time is the output. The paper distinguishes between macroscopic and microscopic evacuation models both of which are able to capture the evacuees' movement over time.
Macroscopic models are mainly used to produce good lower bounds for the evacuation time and do not consider any individual behavior during the emergency situation. These bounds can be used to analyze existing buildings or help in the design phase of planning a building. Macroscopic approaches which are based on dynamic network flow models (minimum cost dynamic flow, maximum dynamic flow, universal maximum flow, quickest path and quickest flow) are described. A special feature of the presented approach is the fact, that travel times of evacuees are not restricted to be constant, but may be density dependent. Using multicriteria optimization priority regions and blockage due to fire or smoke may be considered. It is shown how the modelling can be done using time parameter either as discrete or continuous parameter.
Microscopic models are able to model the individual evacuee's characteristics and the interaction among evacuees which influence their movement. Due to the corresponding huge amount of data one uses simulation approaches. Some probabilistic laws for individual evacuee's movement are presented. Moreover ideas to model the evacuee's movement using cellular automata (CA) and resulting software are presented. In this paper we will focus on macroscopic models and only summarize some of the results of the microscopic approach. While most of the results are applicable to general evacuation situations, we concentrate on building evacuation.
(44 pages, 2001)

25. J. Kuhnert, S. Tiwari

Grid free method for solving the Poisson equation

A Grid free method for solving the Poisson equation is presented. This is an iterative method. The method is based on the weighted least squares approximation in which the Poisson equation is enforced to be satisfied in every iterations. The boundary conditions can also be enforced in the iteration process. This is a local approximation procedure. The Dirichlet, Neumann and mixed boundary value problems on a unit square are presented and the analytical solutions are compared with the exact solutions. Both solutions matched perfectly.
Keywords: Poisson equation, Least squares method, Grid free method
(19 pages, 2001)

26. T. Götz, H. Rave, D. Reinel-Bitzer, K. Steiner, H. Tiemeier

Simulation of the fiber spinning process

To simulate the influence of process parameters to the melt spinning process a fiber model is used and coupled with CFD calculations of the quench air flow. In the fiber model energy, momentum and mass balance are solved for the polymer mass flow. To calculate the quench air the Lattice Boltzmann method is used. Simulations and experiments for different process parameters and hole configurations are compared and show a good agreement.

Keywords: Melt spinning, fiber model, Lattice Boltzmann, CFD

(19 pages, 2001)

27. A. Zemitis

On interaction of a liquid film with an obstacle

In this paper mathematical models for liquid films generated by impinging jets are discussed. Attention is stressed to the interaction of the liquid film with some obstacle. S. G. Taylor [Proc. R. Soc. London Ser. A 253, 313 (1959)] found that the liquid film generated by impinging jets is very sensitive to properties of the wire which was used as an obstacle. The aim of this presentation is to propose a modification of the Taylor's model, which allows to simulate the film shape in cases, when the angle between jets is different from 180°. Numerical results obtained by discussed models give two different shapes of the liquid film similar as in Taylors experiments. These two shapes depend on the regime: either droplets are produced close to the obstacle or not. The difference between two regimes becomes larger if the angle between jets decreases. Existence of such two regimes can be very essential for some applications of impinging jets, if the generated liquid film can have a contact with obstacles.

Keywords: impinging jets, liquid film, models, numerical solution, shape

(22 pages, 2001)

28. I. Ginzburg, K. Steiner

Free surface lattice-Boltzmann method to model the filling of expanding cavities by Bingham Fluids

The filling process of viscoplastic metal alloys and plastics in expanding cavities is modelled using the lattice Boltzmann method in two and three dimensions. These models combine the regularized Bingham model for viscoplastic with a free-interface algorithm. The latter is based on a modified immiscible lattice Boltzmann model in which one species is the fluid and the other one is considered as vacuum. The boundary conditions at the curved liquid-vacuum interface are met without any geometrical front reconstruction from a first-order Chapman-Enskog expansion. The numerical results obtained with these models are found in good agreement with available theoretical and numerical analysis.

Keywords: Generalized LBE, free-surface phenomena, interface boundary conditions, filling processes, Bingham viscoplastic model, regularized models

(22 pages, 2001)

29. H. Neunzert

»Denn nichts ist für den Menschen als Menschen etwas wert, was er nicht mit Leidenschaft tun kann«

Vortrag anlässlich der Verleihung des Akademiepreises des Landes Rheinland-Pfalz am 21.11.2001

Was macht einen guten Hochschullehrer aus? Auf diese Frage gibt es sicher viele verschiedene, fachbezogene Antworten, aber auch ein paar allgemeine Gesichtspunkte: es bedarf der »Leidenschaft« für die Forschung (Max Weber), aus der dann auch die Begeisterung für die Lehre erwächst. Forschung und Lehre gehören zusammen, um die Wissenschaft als lebendiges Tun vermitteln zu können. Der Vortrag gibt Beispiele dafür, wie in angewandter Mathematik Forschungsaufgaben aus praktischen Alltagsproblemstellungen erwachsen, die in die Lehre auf verschiedenen Stufen (Gymnasium bis Graduiertenkolleg) einfließen; er leitet damit auch zu einem aktuellen Forschungsgebiet, der Mehrskalenanalyse mit ihren vielfältigen Anwendungen in Bildverarbeitung, Materialentwicklung und Strömungsmechanik über, was aber nur kurz gestreift wird. Mathematik erscheint hier als eine moderne Schlüsseltechnologie, die aber auch enge Beziehungen zu den Geistes- und Sozialwissenschaften hat.

Keywords: Lehre, Forschung, angewandte Mathematik, Mehrskalenanalyse, Strömungsmechanik

(18 pages, 2001)

30. J. Kuhnert, S. Tiwari

Finite pointset method based on the projection method for simulations of the incompressible Navier-Stokes equations

A Lagrangian particle scheme is applied to the projection method for the incompressible Navier-Stokes equations. The approximation of spatial derivatives is obtained by the weighted least squares method. The pressure Poisson equation is solved by a local iterative procedure with the help of the least squares method. Numerical tests are performed for two dimensional cases. The Couette flow, Poiseuelle flow, decaying shear flow and the driven cavity flow are presented. The numerical solutions are obtained for stationary as well as instationary cases and are compared with the analytical solutions for channel flows. Finally, the driven cavity in a unit square is considered and the stationary solution obtained from this scheme is compared with that from the finite element method.

Keywords: Incompressible Navier-Stokes equations, Meshfree method, Projection method, Particle scheme, Least squares approximation

AMS subject classification: 76D05, 76M28

(25 pages, 2001)

31. R. Korn, M. Krekel

Optimal Portfolios with Fixed Consumption or Income Streams

We consider some portfolio optimisation problems where either the investor has a desire for an a priori specified consumption stream or/and follows a deterministic pay in scheme while also trying to maximize expected utility from final wealth. We derive explicit closed form solutions for continuous and discrete monetary streams. The mathematical method used is classical stochastic control theory.

Keywords: Portfolio optimisation, stochastic control, HJB equation, discretisation of control problems.

(23 pages, 2002)

32. M. Krekel

Optimal portfolios with a loan dependent credit spread

If an investor borrows money he generally has to pay higher interest rates than he would have received, if he had put his funds on a savings account. The classical model of continuous time portfolio optimisation ignores this effect. Since there is obviously a connection between the default probability and the total percentage of wealth, which the investor is in debt, we study portfolio optimisation with a control dependent interest rate. Assuming a logarithmic and a power utility function, respectively, we prove explicit formulae of the optimal control.

Keywords: Portfolio optimisation, stochastic control, HJB equation, credit spread, log utility, power utility, non-linear wealth dynamics

(25 pages, 2002)

33. J. Ohser, W. Nagel, K. Schladitz

The Euler number of discretized sets - on the choice of adjacency in homogeneous lattices

Two approaches for determining the Euler-Poincaré characteristic of a set observed on lattice points are considered in the context of image analysis { the integral geometric and the polyhedral approach. Information about the set is assumed to be available on lattice points only. In order to retain properties of the Euler number and to provide a good approximation of the true Euler number of the original set in the Euclidean space, the appropriate choice of adjacency in the lattice for the set and its background is crucial. Adjacencies are defined using tessellations of the whole space into polyhedrons. In R 3 , two new 14 adjacencies are introduced additionally to the well known 6 and 26 adjacencies. For the Euler number of a set and its complement, a consistency relation holds. Each of the pairs of adjacencies (14:1; 14:1), (14:2; 14:2), (6; 26), and (26; 6) is shown to be a pair of complementary adjacencies with respect to this relation. That is, the approximations of the Euler numbers are consistent if the set and its background (complement) are equipped with this pair of adjacencies. Furthermore, sufficient conditions for the correctness of the approximations of the Euler number are given. The analysis of selected microstructures and a simulation study illustrate how the estimated Euler number depends on the chosen adjacency. It also shows that there is not a uniquely best pair of adjacencies with respect to the estimation of the Euler number of a set in Euclidean space.

Keywords: image analysis, Euler number, neighborhod relationships, cuboidal lattice

(32 pages, 2002)

34. I. Ginzburg, K. Steiner

Lattice Boltzmann Model for Free-Surface flow and Its Application to Filling Process in Casting

A generalized lattice Boltzmann model to simulate free-surface is constructed in both two and three dimensions. The proposed model satisfies the interfacial boundary conditions accurately. A distinctive feature of the model is that the collision processes is carried out only on the points occupied partially or fully by the fluid. To maintain a sharp interfacial front, the method includes an anti-diffusion algorithm. The unknown distribution functions at the interfacial region are constructed according to the first order Chapman-Enskog analysis. The interfacial boundary conditions are satis-

fied exactly by the coefficients in the Chapman-Enskog expansion. The distribution functions are naturally expressed in the local interfacial coordinates. The macroscopic quantities at the interface are extracted from the least-square solutions of a locally linearized system obtained from the known distribution functions. The proposed method does not require any geometric front construction and is robust for any interfacial topology. Simulation results of realistic filling process are presented: rectangular cavity in two dimensions and Hammer box, Campbell box, Sheffield box, and Motorblock in three dimensions. To enhance the stability at high Reynolds numbers, various upwind-type schemes are developed. Free-slip and no-slip boundary conditions are also discussed.
Keywords: Lattice Boltzmann models; free-surface phenomena; interface boundary conditions; filling processes; injection molding; volume of fluid method; interface boundary conditions; advection-schemes; upwind-schemes
(54 pages, 2002)

35. M. Günther, A. Klar, T. Materne, R. Wegener

Multivalued fundamental diagrams and stop and go waves for continuum traffic equations

In the present paper a kinetic model for vehicular traffic leading to multivalued fundamental diagrams is developed and investigated in detail. For this model phase transitions can appear depending on the local density and velocity of the flow. A derivation of associated macroscopic traffic equations from the kinetic equation is given. Moreover, numerical experiments show the appearance of stop and go waves for highway traffic with a bottleneck.
Keywords: traffic flow, macroscopic equations, kinetic derivation, multivalued fundamental diagram, stop and go waves, phase transitions
(25 pages, 2002)

36. S. Feldmann, P. Lang, D. Prätzel-Wolters

Parameter influence on the zeros of network determinants

To a network N(q) with determinant D(s;q) depending on a parameter vector $q \hat{I} R^r$ via identification of some of its vertices, a network N^ (q) is assigned. The paper deals with procedures to find N^ (q), such that its determinant D^ (s;q) admits a factorization in the determinants of appropriate subnetworks, and with the estimation of the deviation of the zeros of D^ from the zeros of D. To solve the estimation problem state space methods are applied.
Keywords: Networks, Equicofactor matrix polynomials, Realization theory, Matrix perturbation theory
(30 pages, 2002)

37. K. Koch, J. Ohser, K. Schladitz

Spectral theory for random closed sets and estimating the covariance via frequency space

A spectral theory for stationary random closed sets is developed and provided with a sound mathematical basis. Definition and proof of existence of the Bartlett spectrum of a stationary random closed set as well as the proof of a Wiener-Khintchine theorem for the power spectrum are used to two ends: First, well known second order characteristics like the covariance can be estimated faster than usual via frequency space. Second, the Bartlett spectrum and the power spectrum can be used as second order characteristics in frequency space. Examples show, that in some cases information about the random closed set is easier to obtain from these characteristics in frequency space than from their real world counterparts.
Keywords: Random set, Bartlett spectrum, fast Fourier transform, power spectrum
(28 pages, 2002)

38. D. d'Humières, I. Ginzburg

Multi-reflection boundary conditions for lattice Boltzmann models

We present a unified approach of several boundary conditions for lattice Boltzmann models. Its general framework is a generalization of previously introduced schemes such as the bounce-back rule, linear or quadratic interpolations, etc. The objectives are two fold: first to give theoretical tools to study the existing boundary conditions and their corresponding accuracy; secondly to design formally third- order accurate boundary conditions for general flows. Using these boundary conditions, Couette and Poiseuille flows are exact solution of the lattice Boltzmann models for a Reynolds number $Re = 0$ (Stokes limit).
Numerical comparisons are given for Stokes flows in periodic arrays of spheres and cylinders, linear periodic array of cylinders between moving plates and for Navier-Stokes flows in periodic arrays of cylinders for $Re < 200$. These results show a significant improvement of the overall accuracy when using the linear interpolations instead of the bounce-back reflection (up to an order of magnitude on the hydrodynamics fields). Further improvement is achieved with the new multi-reflection boundary conditions, reaching a level of accuracy close to the quasi-analytical reference solutions, even for rather modest grid resolutions and few points in the narrowest channels. More important, the pressure and velocity fields in the vicinity of the obstacles are much smoother with multi-reflection than with the other boundary conditions.
Finally the good stability of these schemes is highlighted by some simulations of moving obstacles: a cylinder between flat walls and a sphere in a cylinder.
Keywords: lattice Boltzmann equation, boudary condistions, bounce-back rule, Navier-Stokes equation
(72 pages, 2002)

39. R. Korn

Elementare Finanzmathematik

Im Rahmen dieser Arbeit soll eine elementar gehaltene Einführung in die Aufgabenstellungen und Prinzipien der modernen Finanzmathematik gegeben werden. Insbesondere werden die Grundlagen der Modellierung von Aktienkursen, der Bewertung von Optionen und der Portfolio-Optimierung vorgestellt. Natürlich können die verwendeten Methoden und die entwickelte Theorie nicht in voller Allgemeinheit für den Schulunterricht verwendet werden, doch sollen einzelne Prinzipien so heraus gearbeitet werden, dass sie auch an einfachen Beispielen verstanden werden können.
Keywords: Finanzmathematik, Aktien, Optionen, Portfolio-Optimierung, Börse, Lehrerweiterbildung, Mathematikunterricht
(98 pages, 2002)

40. J. Kallrath, M. C. Müller, S. Nickel

Batch Presorting Problems: Models and Complexity Results

In this paper we consider short term storage systems. We analyze presorting strategies to improve the effiency of these storage systems. The presorting task is called Batch PreSorting Problem (BPSP). The BPSP is a variation of an assigment problem, i. e., it has an assigment problem kernel and some additional constraints. We present different types of these presorting problems, introduce mathematical programming formulations and prove the NP-completeness for one type of the BPSP. Experiments are carried out in order to compare the different model formulations and to investigate the behavior of these models.
Keywords: Complexity theory, Integer programming, Assigment, Logistics
(19 pages, 2002)

41. J. Linn

On the frame-invariant description of the phase space of the Folgar-Tucker equation

The Folgar-Tucker equation is used in flow simulations of fiber suspensions to predict fiber orientation depending on the local flow. In this paper, a complete, frame-invariant description of the phase space of this differential equation is presented for the first time.
Key words: fiber orientation, Folgar-Tucker equation, injection molding
(5 pages, 2003)

42. T. Hanne, S. Nickel

A Multi-Objective Evolutionary Algorithm for Scheduling and Inspection Planning in Software Development Projects

In this article, we consider the problem of planning inspections and other tasks within a software development (SD) project with respect to the objectives quality (no. of defects), project duration, and costs. Based on a discrete-event simulation model of SD processes comprising the phases coding, inspection, test, and rework, we present a simplified formulation of the problem as a multiobjective optimization problem. For solving the problem (i. e. finding an approximation of the efficient set) we develop a multiobjective evolutionary algorithm. Details of the algorithm are discussed as well as results of its application to sample problems.
Key words: multiple objective programming, project management and scheduling, software development, evolutionary algorithms, efficient set
(29 pages, 2003)

43. T. Bortfeld , K.-H. Küfer, M. Monz, A. Scherrer, C. Thieke, H. Trinkaus

Intensity-Modulated Radiotherapy - A Large Scale Multi-Criteria Programming Problem -

Radiation therapy planning is always a tight rope walk between dangerous insufficient dose in the target volume and life threatening overdosing of organs at risk. Finding ideal balances between these inherently contradictory goals challenges dosimetrists and physicians in their daily practice. Today's planning systems are typically based on a single evaluation function that measures the quality of a radiation treatment plan. Unfortunately, such a one dimensional approach can-

not satisfactorily map the different backgrounds of physicians and the patient dependent necessities. So, too often a time consuming iteration process between evaluation of dose distribution and redefinition of the evaluation function is needed.
In this paper we propose a generic multi-criteria approach based on Pareto's solution concept. For each entity of interest - target volume or organ at risk a structure dependent evaluation function is defined measuring deviations from ideal doses that are calculated from statistical functions. A reasonable bunch of clinically meaningful Pareto optimal solutions are stored in a data base, which can be interactively searched by physicians. The system guarantees dynamical planning as well as the discussion of tradeoffs between different entities.
Mathematically, we model the upcoming inverse problem as a multi-criteria linear programming problem. Because of the large scale nature of the problem it is not possible to solve the problem in a 3D-setting without adaptive reduction by appropriate approximation schemes.
Our approach is twofold: First, the discretization of the continuous problem is based on an adaptive hierarchical clustering process which is used for a local refinement of constraints during the optimization procedure. Second, the set of Pareto optimal solutions is approximated by an adaptive grid of representatives that are found by a hybrid process of calculating extreme compromises and interpolation methods.
Keywords: multiple criteria optimization, representative systems of Pareto solutions, adaptive triangulation, clustering and disaggregation techniques, visualization of Pareto solutions, medical physics, external beam radiotherapy planning, intensity modulated radiotherapy
(31 pages, 2003)

44. T. Halfmann, T. Wichmann

Overview of Symbolic Methods in Industrial Analog Circuit Design

Industrial analog circuits are usually designed using numerical simulation tools. To obtain a deeper circuit understanding, symbolic analysis techniques can additionally be applied. Approximation methods which reduce the complexity of symbolic expressions are needed in order to handle industrial-sized problems. This paper will give an overview to the field of symbolic analog circuit analysis. Starting with a motivation, the state-of-the-art simplification algorithms for linear as well as for nonlinear circuits are presented. The basic ideas behind the different techniques are described, whereas the technical details can be found in the cited references. Finally, the application of linear and nonlinear symbolic analysis will be shown on two example circuits.
Keywords: CAD, automated analog circuit design, symbolic analysis, computer algebra, behavioral modeling, system simulation, circuit sizing, macro modeling, differential-algebraic equations, index
(17 pages, 2003)

45. S. E. Mikhailov, J. Orlik

Asymptotic Homogenisation in Strength and Fatigue Durability Analysis of Composites

Asymptotic homogenisation technique and two-scale convergence is used for analysis of macro-strength and fatigue durability of composites with a periodic structure under cyclic loading. The linear damage accumulation rule is employed in the phenomenological micro-durability conditions (for each component of the composite) under varying cyclic loading. Both local and non-local strength and durability conditions are analysed. The strong convergence of the strength and fatigue damage measure as the structure period tends to zero is proved and their limiting values are estimated.
Keywords: multiscale structures, asymptotic homogenization, strength, fatigue, singularity, non-local conditions
(14 pages, 2003)

46. P. Domínguez-Marín, P. Hansen, N. Mladenović, S. Nickel

Heuristic Procedures for Solving the Discrete Ordered Median Problem

We present two heuristic methods for solving the Discrete Ordered Median Problem (DOMP), for which no such approaches have been developed so far. The DOMP generalizes classical discrete facility location problems, such as the p-median, p-center and Uncapacitated Facility Location problems. The first procedure proposed in this paper is based on a genetic algorithm developed by Moreno Vega [MV96] for p-median and p-center problems. Additionally, a second heuristic approach based on the Variable Neighborhood Search metaheuristic (VNS) proposed by Hansen & Mladenovic [HM97] for the p-median problem is described. An extensive numerical study is presented to show the efficiency of both heuristics and compare them.
Keywords: genetic algorithms, variable neighborhood search, discrete facility location
(31 pages, 2003)

47. N. Boland, P. Domínguez-Marín, S. Nickel, J. Puerto

Exact Procedures for Solving the Discrete Ordered Median Problem

The Discrete Ordered Median Problem (DOMP) generalizes classical discrete location problems, such as the N-median, N-center and Uncapacitated Facility Location problems. It was introduced by Nickel [16], who formulated it as both a nonlinear and a linear integer program. We propose an alternative integer linear programming formulation for the DOMP, discuss relationships between both integer linear programming formulations, and show how properties of optimal solutions can be used to strengthen these formulations. Moreover, we present a specific branch and bound procedure to solve the DOMP more efficiently. We test the integer linear programming formulations and this branch and bound method computationally on randomly generated test problems.
Keywords: discrete location, Integer programming
(41 pages, 2003)

48. S. Feldmann, P. Lang

Padé-like reduction of stable discrete linear systems preserving their stability

A new stability preserving model reduction algorithm for discrete linear SISO-systems based on their impulse response is proposed. Similar to the Padé approximation, an equation system for the Markov parameters involving the Hankel matrix is considered, that here however is chosen to be of very high dimension. Although this equation system therefore in general cannot be solved exactly, it is proved that the approximate solution, computed via the Moore-Penrose inverse, gives rise to a stability preserving reduction scheme, a property that cannot be guaranteed for the Padé approach. Furthermore, the proposed algorithm is compared to another stability preserving reduction approach, namely the balanced truncation method, showing comparable performance of the reduced systems. The balanced truncation method however starts from a state space description of the systems and in general is expected to be more computational demanding.
Keywords: Discrete linear systems, model reduction, stability, Hankel matrix, Stein equation
(16 pages, 2003)

49. J. Kallrath, S. Nickel

A Polynomial Case of the Batch Presorting Problem

This paper presents new theoretical results for a special case of the batch presorting problem (BPSP). We will show tht this case can be solved in polynomial time. Offline and online algorithms are presented for solving the BPSP. Competetive analysis is used for comparing the algorithms.
Keywords: batch presorting problem, online optimization, competetive analysis, polynomial algorithms, logistics
(17 pages, 2003)

50. T. Hanne, H. L. Trinkaus

knowCube for MCDM – Visual and Interactive Support for Multicriteria Decision Making

In this paper, we present a novel multicriteria decision support system (MCDSS), called knowCube, consisting of components for knowledge organization, generation, and navigation. Knowledge organization rests upon a database for managing qualitative and quantitative criteria, together with add-on information. Knowledge generation serves filling the database via e. g. identification, optimization, classification or simulation. For "finding needles in haycocks", the knowledge navigation component supports graphical database retrieval and interactive, goal-oriented problem solving. Navigation "helpers" are, for instance, cascading criteria aggregations, modifiable metrics, ergonomic interfaces, and customizable visualizations. Examples from real-life projects, e.g. in industrial engineering and in the life sciences, illustrate the application of our MCDSS.
Key words: Multicriteria decision making, knowledge management, decision support systems, visual interfaces, interactive navigation, real-life applications.
(26 pages, 2003)

51. O. Iliev, V. Laptev

On Numerical Simulation of Flow Through Oil Filters

This paper concerns numerical simulation of flow through oil filters. Oil filters consist of filter housing (filter box), and a porous filtering medium, which completely separates the inlet from the outlet. We discuss mathematical models, describing coupled flows in the pure liquid subregions and in the porous filter media, as well as interface conditions between them. Further, we reformulate the problem in fictitious regions method manner, and discuss peculiarities of the numerical algorithm in solving the coupled system. Next, we show numerical results, validating the model and the

algorithm. Finally, we present results from simulation of 3-D oil flow through a real car filter.
Keywords: oil filters, coupled flow in plain and porous media, Navier-Stokes, Brinkman, numerical simulation
(8 pages, 2003)

52. W. Dörfler, O. Iliev, D. Stoyanov, D. Vassileva

On a Multigrid Adaptive Refinement Solver for Saturated Non-Newtonian Flow in Porous Media

A multigrid adaptive refinement algorithm for non-Newtonian flow in porous media is presented. The saturated flow of a non-Newtonian fluid is described by the continuity equation and the generalized Darcy law. The resulting second order nonlinear elliptic equation is discretized by a finite volume method on a cell-centered grid. A nonlinear full-multigrid, full-approximation-storage algorithm is implemented. As a smoother, a single grid solver based on Picard linearization and Gauss-Seidel relaxation is used. Further, a local refinement multigrid algorithm on a composite grid is developed. A residual based error indicator is used in the adaptive refinement criterion. A special implementation approach is used, which allows us to perform unstructured local refinement in conjunction with the finite volume discretization. Several results from numerical experiments are presented in order to examine the performance of the solver.
Keywords: Nonlinear multigrid, adaptive refinement, non-Newtonian flow in porous media
(17 pages, 2003)

53. S. Kruse

On the Pricing of Forward Starting Options under Stochastic Volatility

We consider the problem of pricing European forward starting options in the presence of stochastic volatility. By performing a change of measure using the asset price at the time of strike determination as a numeraire, we derive a closed-form solution based on Heston's model of stochastic volatility.
Keywords: Option pricing, forward starting options, Heston model, stochastic volatility, cliquet options
(11 pages, 2003)

54. O. Iliev, D. Stoyanov

Multigrid – adaptive local refinement solver for incompressible flows

A non-linear multigrid solver for incompressible Navier-Stokes equations, exploiting finite volume discretization of the equations, is extended by adaptive local refinement. The multigrid is the outer iterative cycle, while the SIMPLE algorithm is used as a smoothing procedure. Error indicators are used to define the refinement subdomain. A special implementation approach is used, which allows to perform unstructured local refinement in conjunction with the finite volume discretization. The multigrid - adaptive local refinement algorithm is tested on 2D Poisson equation and further is applied to a lid-driven flows in a cavity (2D and 3D case), comparing the results with bench-mark data. The software design principles of the solver are also discussed.
Keywords: Navier-Stokes equations, incompressible flow, projection-type splitting, SIMPLE, multigrid methods, adaptive local refinement, lid-driven flow in a cavity
(37 pages, 2003)

55. V. Starikovicius

The multiphase flow and heat transfer in porous media

In first part of this work, summaries of traditional Multiphase Flow Model and more recent Multiphase Mixture Model are presented. Attention is being paid to attempts include various heterogeneous aspects into models. In second part, MMM based differential model for two-phase immiscible flow in porous media is considered. A numerical scheme based on the sequential solution procedure and control volume based finite difference schemes for the pressure and saturation-conservation equations is developed. A computer simulator is built, which exploits object-oriented programming techniques. Numerical result for several test problems are reported.
Keywords: Two-phase flow in porous media, various formulations, global pressure, multiphase mixture model, numerical simulation
(30 pages, 2003)

Status quo: July 2003